Tectonophysics 602 (2013) 153–175

Contents lists available at SciVerse ScienceDirect

Tectonophysics

journal homepage: www.elsevier.com/locate/tecto

Earthquake focal mechanisms, seismogenic stress, and seismotectonics of the Calabrian Arc, Italy

Debora Presti [a,b,*], Andrea Billi [c], Barbara Orecchio [a], Cristina Totaro [a], Claudio Faccenna [b], Giancarlo Neri [a]

[a] Dipartimento di Scienze della Terra, Università di Messina, Messina, Italy
[b] Dipartimento di Scienze Geologiche, Università Roma Tre, Rome, Italy
[c] Consiglio Nazionale delle Ricerche, IGAG, Rome, Italy

ARTICLE INFO

Article history:
Received 23 January 2012
Received in revised form 25 January 2013
Accepted 29 January 2013
Available online 8 February 2013

Keywords:
Calabrian Arc
Earthquake focal mechanism
Seismogenic stress
Seismotectonics
Earthquake catalog

ABSTRACT

Crustal earthquake focal mechanisms are investigated in the Calabrian Arc region, where the western Mediterranean subduction process is close to ending and the residual Ionian subducting slab affected by gravitational roll-back produces a strong variation of faulting regimes at shallow depth along the local section of the convergent margin. An updated database of earthquake focal mechanisms has been compiled by selecting the best-quality solutions available in the literature and in catalogs, and by adding 17 new solutions estimated in the present work. A total of 164 mechanisms are included in this database, 142 computed by waveform inversion and 22 by analysis of P-wave first motions from earthquakes with good network coverage and no less than 14 records. 60% of the solutions included in the database have never been used for regional-scale geodynamic investigations before the present study, and this makes the compiled database substantially new for our application. Focal mechanisms have been inverted for stress tensor orientations to obtain the principal stress axes over the study region. Results are compatible with three major tectonic domains subject to markedly different regional stresses along the arc. These three domains are separated by two transitional domains, which are located on top of the Ionian subducting slab edges and are likely forced in their horizontal transfer kinematics by the different tectonic regimes occurring in the adjacent major domains rather than by the regional tectonics. This along-arc differential tectonics is at least in part interpreted as the surface expression of the different deep mechanisms occurring in correspondence of the narrow Ionian slab and their lateral edges. Open tectonic questions are emphasized and proposed for future studies.

1. Introduction

Since their first processing, earthquake focal mechanisms have been revealed as fundamental in the study of the relationship between earthquakes, seismic faults, and active tectonics (Anderson et al., 1993; Dziewonski et al., 1981; Ekström and England, 1989; Ekström et al., 2005; Grimison and Chen, 1986; Jackson and McKenzie, 1988; McCaffrey et al., 1985). Focal mechanisms have been revealed as essential also in other tectonic studies such as the determination of the true sense of motion along transform faults across oceanic spreading ridges (Sykes, 1967; Wilson, 1965) or the discovery that subducting slabs may be under compression, under tension, or both in different sectors (Isacks and Molnar, 1971). Moreover, the determination of earthquake focal mechanisms is the prerequisite for computing the seismogenic stress of a region and compiling related maps of active stress (Barba et al., 2010; Gephart and Forsyth, 1984; McKenzie, 1969; Montone et al., 2004; Zoback, 1983; Zoback and Zoback, 1980), which, in addition to the study of deformation zones and related geodynamic engines, have been also used for probability maps of future earthquakes (e.g., Cinti et al., 2004) as well as for hydrocarbon field development and well planning (e.g., Lindholm et al., 1995). The rapid determination of earthquake source parameters may be also crucial for prompt rescues in the case of destructive earthquakes (Scognamiglio et al., 2010).

Although earthquake focal mechanisms have been revealed as a very powerful tool in seismotectonic studies, the reliability of these data may decrease for low magnitude earthquakes ($M<4$). Moreover, the determination of focal mechanisms is obviously limited to the temporal range of earthquake instrumental recording, with a dramatic drop of reliability for the first decades of the instrumental epoch, when the world seismic network was still poorly developed and recording equipments were rudimentary.

Focal mechanisms elaborated by using P-wave first motions may be biased by an inadequate coverage of seismic stations, whereas those elaborated by waveform analyses have so far demonstrated as being much more stable and reliable (e.g., Lay and Wallace, 1995; Pondrelli et al., 2006; Scognamiglio et al., 2009). This is the case, for instance, of at least a portion of southern Italy, where the substantial lack of offshore

* Corresponding author at: Dipartimento di Scienze della Terra, Università di Messina, Salita Sperone 31, Messina-Sant'Agata, 98166, Italy. Tel.: +39 0906765102.
E-mail address: dpresti@unime.it (D. Presti).

0040-1951/$ – see front matter
http://dx.doi.org/10.1016/j.tecto.2013.01.030

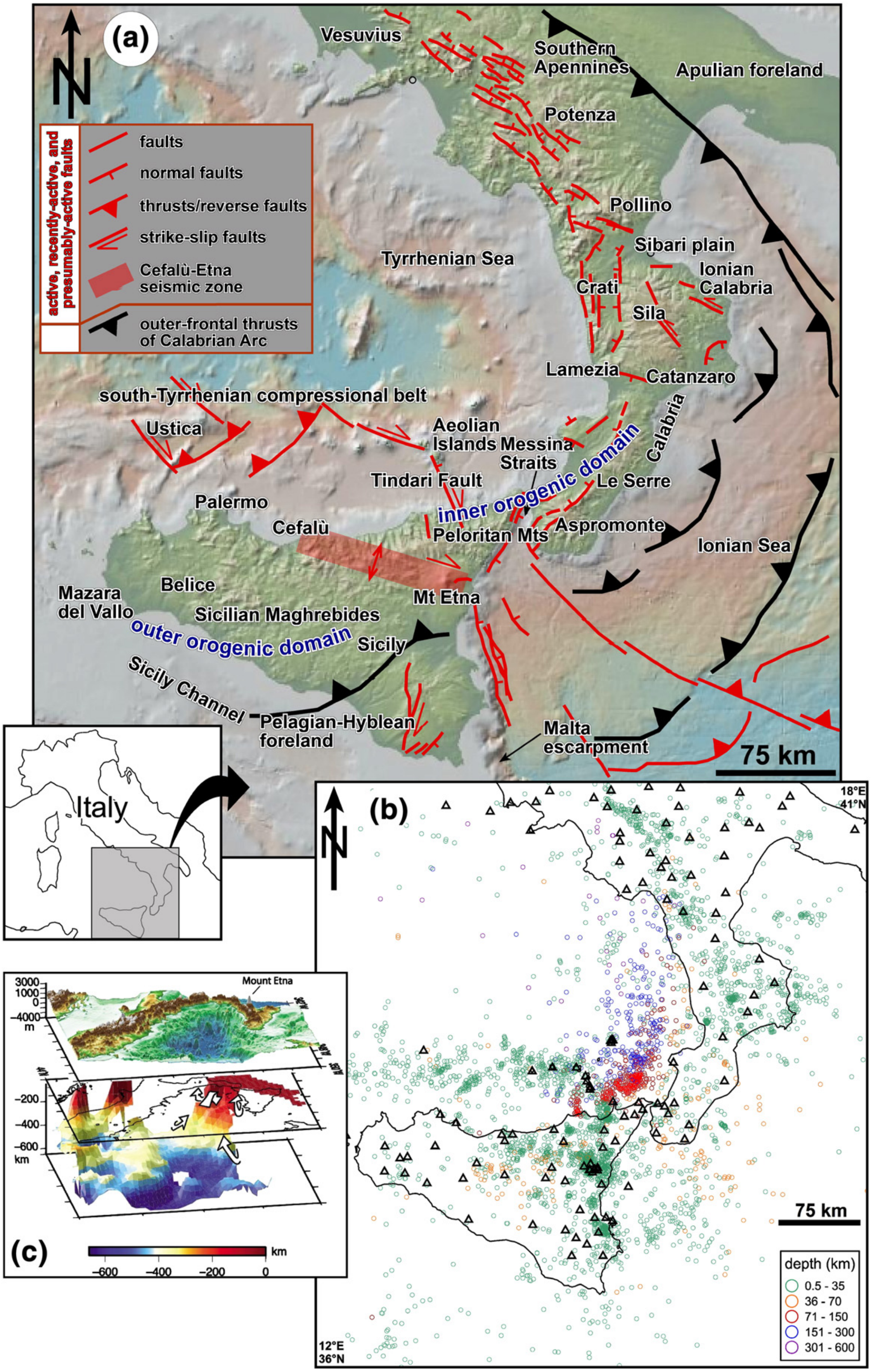
(a)
N
active, recently-active, and presumably-active faults
faults
normal faults
thrusts/reverse faults
strike-slip faults
Cefalù-Etna seismic zone
outer-frontal thrusts of Calabrian Arc
Vesuvius
Southern Apennines
Apulian foreland
Potenza
Pollino
Sibari plain
Ionian Calabria
Tyrrhenian Sea
Crati
Sila
Lamezia
Catanzaro
Calabria
south-Tyrrhenian compressional belt
Ustica
Aeolian Islands
Messina Straits
inner orogenic domain
Tindari Fault
Le Serre
Palermo
Cefalù
Peloritan Mts
Aspromonte
Ionian Sea
Belice
Mt Etna
Mazara del Vallo
Sicilian Maghrebides
outer orogenic domain
Sicily
Sicily Channel
Pelagian-Hyblean foreland
Malta escarpment
75 km
Italy
(b)
18°E 41°N
12°E 36°N
75 km
depth (km)
0.5 - 35
36 - 70
71 - 150
151 - 300
301 - 600
(c)
Mount Etna
3000
1000
0
-4000
m
-200
-400
-600
km
-600
-400
-200
0
km

stations may significantly bias the determination of earthquake focal mechanisms through P-wave first motions (Barberi et al. 2006; D'Amico et al., 2010; Neri et al. 2003; Pondrelli et al., 2006). It follows that continuous processing and improvements of earthquake focal mechanisms are necessary to increase their reliability and to expand the temporal and magnitude range of focal mechanism databases.

The Calabrian Arc in southern Italy (Fig. 1) is the result of the Neogene–Quaternary tectonic convergence between Africa (Nubia) and Europe in the central Mediterranean (Billi et al., 2011; Carminati et al., 2012; Catalano and D'Argenio, 1978; Chiarabba et al., 2005; Dewey et al., 1989; Faccenna et al., 2004; Gueguen et al., 1998; Malinverno and Ryan, 1986; Pepe et al., 2010; Rosenbaum and Lister, 2004). This curved structure is characterized by very heterogeneous seismotectonic regimes along its length (Cristofolini et al., 1985; Montone et al., 2004) and has been the site of destructive, magnitude class 6 and 7 earthquakes that occurred both in recent and historical times (Galli et al., 2008; Neri et al., 2006). The tectonic picture of the Calabrian Arc is complicated by the presence of a narrow subducting slab beneath Calabria (Fig. 1c; Dvorkin et al., 1993; Neri et al., 2009; Selvaggi and Chiarabba, 1995), of two active volcanic districts, one in eastern Sicily (Mt Etna) and another one in southeastern Tyrrhenian (Aeolian Islands) (Barberi et al., 1974; Carminati et al., 2010; Lustrino et al., 2011; Peccerillo, 2003), of rapidly uplifting areas in Calabria and eastern Sicily (Antonioli et al., 2006; Faccenna et al., 2011), and of diverging GPS velocity vectors across the Messina Straits (D'Agostino and Selvaggi, 2004; Palano et al., 2012; Serpelloni et al., 2010). Despite years of seismotectonic studies of this region, the causative faults of several destructive recent and historical earthquakes are still unknown or debated (e.g., Billi et al., 2010a; Galli et al., 2008) as are the location, geometry, and kinematics of the structures marking the transition between adjacent seismotectonic domains characterized by different seismic regimes (Goes et al., 2004).

In this paper, within the framework of the TOPO-EUROPE research program (Cloetingh et al., 2007, 2009, 2011), we provide an updated database (Table 1) of crustal earthquake focal mechanisms for the Calabrian Arc determined by waveform analyses (142 events). We include also 22 selected focal mechanisms determined through P-wave first motions from earthquakes of the Southern Apennines as these mechanisms are particularly reliable for number of polarities (≥14), seismic network coverage, and other quality parameters such as the Q_p and Q_f factors of the FPFIT standard algorithm indicating the solution uniqueness and the misfit of polarity data, respectively. We inverted data from our database to compute the seismogenic stress of various domains in the study region. The integration, within this up-to-date database, of earthquake focal mechanisms determined using the Cut and Paste method (CAP) has made it possible to expand the database of focal mechanisms from waveform analysis down to a minimum of magnitude 2.6 without overlooking the reliability of results (Chevrot et al., 2011; D'Amico et al., 2010; Zhao and Helmberger, 1994; Zhu and Helmberger, 1996). We have also performed stability tests on these focal mechanisms and some of these tests are presented below. In our database, 17 focal mechanisms out of a total of 164 are new, whereas the other ones are selected (see below the selection criteria) from literature and catalogs (Table 1). These latter mechanisms, however, have not been so far extensively used for seismotectonic purposes, in particular this is the first time in which the solutions included in our database are used in a general seismotectonic study of the Calabrian Arc region. We used the database compiled for this paper and the derived seismogenic stresses to improve the knowledge of the seismotectonics of the Calabrian Arc and to emphasize unsolved or poorly understood tectonic problems to be addressed in the future, possibly through the integration of our database with new geodetic, paleoseismological, and other neotectonic data.

2. Tectonic setting

2.1. Surface and shallow setting

The large Calabrian Arc is a Cenozoic–Quaternary curved orogen (Fig. 1a) running from the NW–SE-trending Southern Apennines to the E–W-trending Sicilian Maghrebides (Carminati et al., 2012; Catalano and D'Argenio, 1978; Catalano et al., 1996; Cifelli et al., 2008; Faccenna et al., 2004; Gueguen et al., 1998; Lavecchia et al., 2007a; Malinverno and Ryan, 1986; Mariotti and Doglioni, 2000; Mattei et al., 2004, 2007; Minelli and Faccenna, 2010; Patacca and Scandone, 2007; Polonia et al., 2011; Rosenbaum and Lister, 2004; Scrocca et al., 2007). The central part of the Calabrian Arc is located on top of a narrow subduction zone (Fig. 1c), whose activity is now close to cessation (Neri et al., 2009), but still slowly retreating (D'Agostino et al., 2011). The Neogene–Quaternary evolution, southeastward migration, and curvature development of the Calabrian Arc have been all controlled by the migration and rollback, respectively, of the subduction zone and Ionian slab, a fragment of oceanic lithosphere between the continental domains of Adria, to the northeast, and Africa, to the west (Ascione et al., 2012; Carminati et al., 1998; Faccenna et al., 2001, 2005; Gvirtzman and Nur, 1999, 2001; Malinverno and Ryan, 1986; Scrocca et al., 2005; Spakman and Wortel 2004; Wortel and Spakman, 2000). The Calabrian Arc consists of two main orogenic domains: (1) the outer domain, including the Southern Apennines and Sicilian Maghrebides, and (2) the inner domain, including the Calabro-Peloritan belt, which occupies the regions of Calabria, northeastern Sicily, and part of southern Tyrrhenian.

The outer domain is mainly composed of deformed Meso-Cenozoic platform and basin sediments derived from the margins of the African and Adriatic continents and from the Neogene–Quaternary foredeep and thrust-top basins. Contractional phases in Southern Apennines and Sicilian Maghrebides started in late Miocene time and lasted until early Pleistocene time as demonstrated by lower Pleistocene sediments suturing the outer front of the thrust-fold belt in the Sicily Channel (Butler and Grasso, 1993). Contraction may indeed be still active as demonstrated, for instance, by the 1968 Belice earthquake in central-western Sicily (Monaco et al., 1996; Lavecchia et al., 2007a, 2007b; see also Speranza et al., 1999, for rotational deformations up to Pleistocene–Holocene time). Post-orogenic extension followed the contractional phases since late Pliocene time in Southern Apennines, where this tectonic regime is still active (Montone et al., 2004).

The inner domain of the Calabrian Arc is mainly composed of crystalline and metamorphic rocks overlain by the Mesozoic sedimentary cover. These units are, in places, unconformably overlain by Neogene sedimentary sequences. The inner units drifted away toward southeast from the Sardinia–Corsica block during early Miocene time and accreted onto the outer domain of the Calabrian Arc (Alvarez et al., 1974; Bonardi et al., 2001; Olivetti et al., 2010; Vignaroli et al., 2008). Most of this tectonic edifice was subsequently (since late Tortonian time; Pepe et al., 2000) stretched apart during the extensional phases that led to the formation of the Tyrrhenian back-arc domain.

For what concerns the present time, recent GPS data show a rather heterogeneous velocity field along the Calabrian Arc (Billi et al., 2011; Cuffaro et al., 2011; D'Agostino and Selvaggi, 2004; D'Agostino et al.,

Fig. 1. (a) Tectonic map of the Calabrian Arc, southern Italy, showing the main known active, recently-active, or presumably-active faults and seismic zones (red symbols), as well as the main outer and frontal thrusts of the Calabrian Arc (black symbols). Data are from several papers cited in the text. The extensional Cefalù–Etna seismic zone is collectively represented with a shaded rectangle because active fault segments in this zone are small and uncertain. (b) Map of the earthquake epicenters for the Calabrian Arc (June 2005–June 2011, M ≥ 2.0). Colors are for different focal depths. Triangles represent seismic stations. Data are from the Italian Seismic Instrumental and parametric database (ISIDE, http://iside.rm.ingv.it/iside/standard/index.jsp). (c) Three-dimensional view of the Tyrrhenian area and Calabrian Arc (view from NNW) and reconstruction (based on tomographic data) of the narrow slab beneath Calabria (after Faccenna et al., 2011; Billi et al., 2011). Arrows indicate the pattern of mantle flow expected on the sides and on top of the narrow subducting Ionian slab.

Table 1
Main parameters of earthquakes reported in Fig. 4.

ID	Year	Mn	Day	O.T.	Lon	Lat	Depth	Strike	Dip	Rake	Mag	M-Type	Source	Method	P_az	P_pl	T_az	T_pl	FT
1	1977	6	5	13:59:22.5	14.46	37.84	11.3	61	26	−139	4.6	Mw	ItCMT	Wf Inv	230	57	7	26	NF
2	1978	3	11	19:20:49.1	16.03	38.10	33.0	270	41	−72	5.6	Mb	ItCMT	Wf Inv	281	77	167	5	NF
3	1978	4	15	23:33:47.2	15.07	38.39	14.0	135	60	−176	5.5	Mb	ItCMT	Wf Inv	355	23	93	18	SS
4	1979	1	20	13:49:59.0	12.86	38.67	9.0	72	29	53	5.2	Mb	ItCMT	Wf Inv	9	20	232	63	TF
5	1980	2	20	02:34:02.9	16.21	39.30	12.0	14	43	−78	4.8	Mb	ItCMT	Wf Inv	23	81	276	3	NF
6	1980	3	9	12:03:40.0	16.12	39.94	19.0	157	35	−80	4.6	Mb	ItCMT	Wf Inv	210	78	60	10	NF
7	1980	5	14	01:41:03.8	15.85	40.46	24.0	119	38	−112	4.5	Mb	ItCMT	Wf Inv	282	74	45	9	NF
8	1980	5	28	19:51:19.3	14.25	38.48	14.0	83	43	99	5.7	Mb	ItCMT	Wf Inv	347	2	97	83	TF
9	1980	6	1	02:32:52.5	14.33	38.39	10.0	65	39	91	4.9	Mb	ItCMT	Wf Inv	334	6	148	84	TF
10	1980	11	23	18:34:53.8	15.37	40.91	10.0	135	41	−80	6.9	Ms	ItCMT	Wf Inv	162	82	38	4	NF
11	1980	11	24	00:23:59.5	15.26	40.89	10.0	131	29	−110	4.9	Mb	ItCMT	Wf Inv	266	70	56	17	NF
12	1980	11	24	03:03:53.7	15.33	40.90	10.0	115	44	−125	5.1	Mb	ItCMT	Wf Inv	305	66	49	6	NF
13	1980	11	25	18:28:21.5	15.40	40.65	10.0	129	26	−65	4.9	Mb	ItCMT	Wf Inv	171	66	20	21	NF
14	1980	11	25	17:06:44.0	15.47	40.70	10.0	122	30	−119	5.1	Mb	ItCMT	Wf Inv	274	67	53	18	NF
15	1980	12	3	23:54:24.2	15.48	40.74	10.0	148	36	−76	4.9	Mb	ItCMT	Wf Inv	187	77	48	10	NF
16	1981	1	16	00:37:46.8	15.37	40.95	15.0	115	30	−93	5.0	Mb	ItCMT	Wf Inv	213	75	27	15	NF
17	1981	6	7	13:00:56.6	12.47	37.67	18.0	48	29	48	4.9	Mb	ItCMT	Wf Inv	349	21	214	61	TF
18	1981	6	22	09:36:18.0	14.09	38.49	13.0	71	47	116	4.8	Mb	ItCMT	Wf Inv	323	1	56	71	TF
19	1981	11	29	05:06:47.0	15.64	40.74	33.0	104	41	−138	4.9	Mb	ItCMT	Wf Inv	295	58	47	13	NF
20	1982	3	21	09:44:00.5	15.64	39.70	18.9	15	39	−127	5.0	Mb	ItCMT	Wf Inv	196	65	311	11	NF
21	1982	8	15	15:09:49.9	15.36	40.81	10.0	158	48	−45	4.8	Mb	ItCMT	Wf Inv	137	58	38	6	NF
22	1987	1	28	05:33:21.9	15.47	40.95	10.0	160	45	−79	4.6	Mb	ItCMT	Wf Inv	156	82	62	1	NF
23	1987	8	13	07:22:09.5	15.06	37.90	35.9	352	42	−10	4.8	Mb	ItCMT	Wf Inv	323	37	211	26	U
24	1988	1	8	13:05:46.5	16.01	40.08	10.0	148	30	−86	4.8	Mb	ItCMT	Wf Inv	227	75	55	15	NF
25	1990	5	5	07:21:19.4	15.85	40.75	26.0	184	73	13	5.3	Mb	ItCMT	Wf Inv	147	0	237	10	SS
26	1990	5	5	07:38:12.3	15.81	40.75	15.0	282	83	173	5.0	Mb	ItCMT	Wf Inv	138	3	46	21	SS
27	1990	10	29	08:16:14.1	14.67	36.23	23.0	198	72	−13	4.5	Mb	ItCMT	Wf Inv	156	22	64	4	SS
28	1990	12	13	00:24:24.3	15.50	37.20	10.0	274	64	174	5.4	Mb	ItCMT	Wf Inv	138	14	233	22	SS
29	1991	5	26	12:26:00.3	15.77	40.73	8.0	183	71	−9	5.2	Mb	ItCMT	Wf Inv	141	20	48	7	SS
30	1992	4	6	13:08:34.0	14.61	37.83	21.0	100	37	−97	4.7	Mb	ItCMT	Wf Inv	223	81	15	8	NF
31	1993	6	26	17:47:53.8	14.21	37.92	10.0	170	53	6	4.4	Mb	ItCMT	Wf Inv	129	22	26	29	U
32	1995	5	29	06:52:27.3	12.07	37.90	11.0	82	70	−180	4.8	Mb	ItCMT	Wf Inv	305	14	39	14	SS
33	1996	4	3	13:04:34.5	15.49	40.76	10.0	123	30	−110	4.9	Mb	ItCMT	Wf Inv	260	71	48	16	NF
34	1996	12	14	00:18:44.9	13.84	37.81	40.0	123	23	−43	4.7	Mb	ItCMT	Wf Inv	141	57	357	28	NF
35	1997	3	25	00:46:13.8	16.03	36.93	33.0	104	78	179	4.7	Mb	ItCMT	Wf Inv	328	8	60	9	SS
36	1998	1	17	12:32:51.2	12.90	38.40	10.0	58	29	71	3.5	Ms	ItCMT	Wf Inv	342	17	192	70	TF
37	1998	6	20	02:25:47.0	13.08	38.46	10.0	69	22	76	4.9	Mb	ItCMT	Wf Inv	350	23	184	66	TF
38	1998	6	21	08:59:47.0	13.10	38.50	10.0	69	36	77	4.3	Mb	ItCMT	Wf Inv	348	10	207	78	TF
39	1998	6	21	12:59:04.0	12.67	38.43	10.0	88	38	102	4.5	Mb	ItCMT	Wf Inv	349	8	125	79	TF
40	1998	9	9	11:27:59.3	15.98	40.03	10.0	139	29	−83	5.2	Mb	ItCMT	Wf Inv	211	73	44	16	NF
41	1998	9	14	05:24:47.0	13.60	38.46	10.0	72	30	80	4.4	Ms	ItCMT	Wf Inv	349	15	188	74	TF
42	1999	2	14	11:45:54.0	15.06	38.17	33.0	18	39	−108	4.5	Mb	ItCMT	Wf Inv	178	77	301	7	NF
43	2001	4	22	13:56:35.5	15.10	37.72	10.0	316	56	27	5.1	Mb	ItCMT	Wf Inv	265	7	169	41	TS
44	2001	5	26	06:02:20.0	16.34	37.46	33.0	71	54	134	4.8	Mb	ItCMT	Wf Inv	312	0	42	56	TF
45	2001	10	18	11:02:44.0	16.61	39.10	10.0	332	44	−88	4.1	Mb	ItCMT	Wf Inv	7	88	241	1	NF
46	2001	11	25	19:34:19.5	13.96	37.91	20.0	137	31	−57	4.3	Mb	ItCMT	Wf Inv	158	66	23	17	NF
47	2001	12	9	12:15	15.29	40.80	16.6	130	20	−80	3.3	Ml	Maggi&Al	Pol	203	65	32	25	NF
48	2002	4	2	04:22	15.89	40.27	13.7	165	85	−100	2.7	Ml	Maggi&Al	Pol	64	49	264	39	U
49	2002	4	5	04:52:23.5	14.74	38.48	10.0	90	41	108	4.1	Mb	ItCMT	Wf Inv	347	5	101	77	TF
50	2002	4	17	06:42:54.3	16.84	39.70	5.0	121	38	−7	4.7	Mb	ItCMT	Wf Inv	93	38	337	30	U
51	2002	4	18	20:56:47.6	15.58	40.69	10.0	340	49	−52	4.4	Mb	ItCMT	Wf Inv	319	62	224	2	NF
52	2002	5	8	19:29	15.99	40.09	14.5	280	85	−130	2.9	Ml	Maggi&Al	Pol	155	37	41	29	U
53	2002	6	11	20:02	15.72	40.52	14.0	140	50	−130	2.1	Ml	Maggi&Al	Pol	343	60	77	2	NF
54	2002	6	18	23:31	15.76	40.53	11.0	255	75	0	2.3	Ml	Maggi&Al	Pol	211	11	119	11	SS
55	2002	9	3	01:45	15.69	40.50	14.8	85	65	−130	1.9	Ml	Maggi&Al	Pol	307	52	203	11	NF
56	2002	9	6	01:21:28.6	13.70	38.38	5.0	26	50	40	5.8	Mb	ItCMT	Wf Inv	329	6	231	53	TF
57	2002	9	6	01:45:30.3	13.73	38.44	4.0	252	48	126	4.5	Mb	ItCMT	Wf Inv	137	3	233	64	TF
58	2002	9	10	02:32:51.3	13.70	38.47	5.0	71	29	126	4.0	Mb	ItCMT	Wf Inv	315	20	92	64	TF
59	2002	9	20	23:06:03.8	13.74	38.46	5.0	46	33	77	4.5	Mb	ItCMT	Wf Inv	325	13	176	76	TF
60	2002	9	27	06:10:44.9	13.69	38.44	5.0	41	39	70	4.8	Mb	ItCMT	Wf Inv	325	8	205	75	TF
61	2002	9	28	02:46:46.3	13.71	38.47	5.0	79	39	103	4.6	Mb	ItCMT	Wf Inv	340	7	109	79	TF
62	2002	10	2	22:57:25.9	13.72	38.46	15.0	33	41	59	4.9	Mw	ItCMT	Wf Inv	325	8	214	69	TF
63	2002	10	4	22:58	15.93	40.25	10.8	320	85	10	2.9	Ml	Maggi&Al	Pol	94	3	185	11	SS
64	2002	10	27	02:50:26.2	15.16	37.79	10.0	320	60	171	4.6	Mb	ItCMT	Wf Inv	184	15	281	27	SS
65	2002	10	27	07:32:08.7	15.18	37.92	10.0	67	54	19	4.4	Mb	ItCMT	Wf Inv	20	13	280	37	SS
66	2002	10	29	10:02:21.5	15.27	37.67	10.0	316	61	−173	4.4	Mb	ItCMT	Wf Inv	175	25	273	16	SS
67	2002	10	29	16:39:47.5	15.56	37.69	10.0	207	54	−28	4.1	Mb	ItCMT	Wf Inv	176	43	78	8	NS
68	2002	11	30	01:19	15.91	40.23	10.6	120	40	−80	2.4	Ml	Maggi&Al	Pol	153	82	23	5	NF
69	2003	7	7	15:08:12.0	14.90	36.01	10.0	350	62	4	4.8	Mb	ItCMT	Wf Inv	307	17	210	22	SS
70	2004	9	3	00:04	15.64	40.69	21.9	80	55	160	4.1	Ml	Maggi&Al	Pol	307	12	46	37	SS
71	2004	10	11	07:31:41.0	15.48	37.88	6.6	89	90	−45	3.6	Mw	CAP-PEPI	Wf Inv	34	30	144	30	U
72	2004	10	22	21:10:13.0	15.32	38.08	10.7	78	61	−37	3.4	Mw	CAP-PEPI	Wf Inv	42	46	134	2	NS
73	2005	1	31	10:44:50.0	16.86	39.66	30.0	23	79	−41	4.1	Mw	CAP-BGTA	Wf Inv	334	36	79	19	SS
74	2005	4	19	22:36:23.0	15.66	38.14	7.1	220	42	−10	3.1	Mw	CAP-PEPI	Wf Inv	191	37	79	26	U
75	2005	4	23	19:11:43.0	16.71	39.47	23.0	128	58	14	4.1	Mw	CAP-BGTA	Wf Inv	83	13	345	31	SS
76	2005	4	23	19:10:48.0	15.82	38.43	13.6	120	50	−64	2.8	Mw	CAP-PEPI	Wf Inv	97	70	192	2	NF

Table 1 (*continued*)

ID	Year	Mn	Day	O.T.	Lon	Lat	Depth	Strike	Dip	Rake	Mag	M-Type	Source	Method	P_az	P_pl	T_az	T_pl	FT
77	2005	6	2	03:05:50.6	15.31	39.59	7.0	278	73	−172	3.7	Mw	CAP-BSSA	Wf Inv	141	18	233	6	SS
78	2005	7	21	15:41:42.6	14.85	39.40	7.0	184	68	41	3.8	Mw	CAP-BSSA	Wf Inv	307	10	46	44	TS
79	2005	8	18	22:02:27.0	15.12	37.80	6.7	82	50	−18	3.1	Mw	CAP-PEPI	Wf Inv	51	38	307	17	SS
80	2005	9	7	12:40:33.0	16.32	38.71	16.0	80	90	−42	3.6	Mw	CAP-BGTA	Wf Inv	27	28	133	28	U
81	2005	9	27	22:33:09.3	17.10	38.62	29.0	38	79	141	3.9	Mw	CAP-BSSA	Wf Inv	93	18	350	35	SS
82	2005	10	30	19:09:46.8	15.93	38.53	15.0	208	32	−139	3.5	Mw	CAP-BSSA	Wf Inv	26	58	153	21	NF
83	2005	11	18	18:35:25.0	17.07	39.17	23.0	120	34	3	3.6	Mw	CAP-BGTA	Wf Inv	89	34	327	37	U
84	2005	12	3	08:33:01.8	17.00	39.20	15.0	290	64	−18	3.8	Mw	CAP	Wf Inv	251	30	157	7	SS
85	2006	2	27	04:34:01.0	15.17	38.10	10.1	62	50	−71	4.1	Mw	CAP-PEPI	Wf Inv	36	75	139	3	NF
86	2006	2	27	09:11:59.0	15.18	38.14	10.5	39	48	−90	3.1	Mw	CAP-PEPI	Wf Inv	82	61	331	11	NF
87	2006	2	27	14:16:06.0	15.18	38.14	9.1	76	48	−58	3.1	Mw	CAP-PEPI	Wf Inv	58	67	324	2	NF
88	2006	3	29	20:20:00.0	13.89	37.73	10.0	338	80	−42	3.9	Mw	TDMT	Wf Inv	289	36	34	20	SS
89	2006	4	17	02:44:06.0	17.05	39.61	28.0	114	74	−3	4.4	Mw	CAP-BGTA	Wf Inv	71	13	338	9	SS
90	2006	4	23	14:42:38.0	15.02	37.04	24.0	100	88	147	3.9	Mw	TDMT	Wf Inv	151	21	51	24	U
91	2006	5	20	07:05:56.0	14.95	37.65	12.0	280	75	47	3.7	Mw	TDMT	Wf Inv	41	18	149	43	TS
92	2006	6	22	19:34:58.0	16.63	39.73	30.0	151	42	81	4.6	Mw	CAP-BGTA	Wf Inv	67	3	308	83	TF
93	2006	7	2	17:52:00.0	15.10	38.13	10.0	70	59	−49	2.6	Mw	CAP-PEPI	Wf Inv	34	55	132	5	NF
94	2006	7	18	07:42:40.0	15.17	38.12	9.1	90	41	−48	3.1	Mw	CAP-PEPI	Wf Inv	82	61	331	11	NF
95	2006	9	7	15:31:43.0	16.19	40.57	34.0	178	55	35	4.0	Mb	ItCMT	Wf Inv	124	4	29	48	TS
96	2006	9	26	16:26	15.46	40.72	7.8	80	75	−110	3.0	Ml	Maggi&Al	Pol	325	56	186	27	NF
97	2006	10	6	21:16:23.0	15.57	38.10	9.6	18	52	−90	3.2	Mw	CAP-PEPI	Wf Inv	288	83	108	7	NF
98	2006	11	4	05:59:22.0	15.01	38.03	10.6	59	49	−36	3.0	Mw	CAP-PEPI	Wf Inv	34	51	294	9	NS
99	2006	11	24	04:37:40.0	15.76	36.26	11.0	188	82	0	4.7	Mb	ItCMT	Wf Inv	143	6	53	6	SS
100	2006	12	19	14:58:06.5	14.91	37.78	23.0	18	16	−40	4.1	Mb	ItCMT	Wf Inv	42	54	247	34	NF
101	2007	3	26	13:55:25.0	17.04	39.26	10.0	297	55	−15	4.1	Mw	ItCMT	Wf Inv	262	34	162	15	SS
102	2007	4	10	19:17:23.0	12.84	36.96	29.7	100	75	164	4.1	Mw	TDMT	Wf Inv	147	0	57	22	SS
103	2007	4	26	00:49:36.0	16.35	39.55	13.0	231	22	−23	3.9	Mw	CAP-BGTA	Wf Inv	230	49	90	34	U
104	2007	5	17	05:48:13.1	14.69	38.57	8.0	22	50	8	3.5	Mw	CAP	Wf Inv	341	22	236	32	U
105	2007	5	25	09:39:45.0	16.83	39.67	25.0	91	29	−48	4.2	Mw	CAP-BGTA	Wf Inv	105	61	330	21	NF
106	2007	6	15	22:56:01.0	15.29	36.97	18.0	12	87	20	3.6	Ml	TDMT	Wf Inv	145	12	238	16	SS
107	2007	6	17	12:11:58.0	15.79	38.37	10.0	262	38	−43	2.9	Mw	CAP-PEPI	Wf Inv	256	59	140	15	NF
108	2007	7	14	18:13:02.7	14.75	38.63	4.0	30	31	38	3.1	Mw	CAP	Wf Inv	337	22	209	56	TF
109	2007	7	14	02:27	15.72	40.5	20.22	105	5	−100	2.6	Ml	Frepoli&Al	Pol	206	50	24	40	U
110	2007	8	1	00:07:54.0	17.20	39.02	40.0	80	67	−45	4.1	Mw	CAP-BGTA	Wf Inv	38	47	139	11	NS
111	2007	8	18	14:04:07.0	15.13	38.23	9.4	44	50	−23	3.9	Mw	CAP-PEPI	Wf Inv	15	42	272	14	NS
112	2007	8	18	14:21:11.0	15.12	38.19	10.0	26	69	18	3.4	Mw	CAP-PEPI	Wf Inv	338	3	247	27	SS
113	2007	9	23	07:12:46.2	14.79	38.59	8.0	27	60	28	3.6	Mw	CAP	Wf Inv	336	4	243	40	U
114	2007	9	30	15:41:20.0	14.80	38.59	6.0	70	73	16	3.1	Mw	CAP	Wf Inv	23	1	292	23	SS
115	2008	1	18	13:01:00.0	16.55	39.15	15.5	57	78	−67	3.9	Mw	TDMT	Wf Inv	353	52	129	29	NF
116	2008	1	20	20:55	15.97	40.52	11.16	345	35	−100	2.2	Ml	Frepoli&Al	Pol	112	78	262	10	NF
117	2008	2	9	07:46:36.0	15.56	37.84	6.9	40	90	−10	3.0	Mw	CAP-PEPI	Wf Inv	355	7	85	7	SS
118	2008	2	21	05:00:08.7	17.97	37.82	30.0	333	27	134	4.5	Mb	ItCMT	Wf Inv	211	24	348	59	TF
119	2008	3	10	10:33:27.2	16.84	39.65	20.0	121	39	−7	3.5	Mw	CAP	Wf Inv	93	37	337	30	U
120	2008	4	8	17:20:03.1	16.66	39.16	10.0	235	49	−35	4.0	Mb	ItCMT	Wf Inv	210	50	109	9	NS
121	2008	4	13	13:06:57.0	15.70	38.25	14.3	6	47	−36	2.8	Mw	CAP-PEPI	Wf Inv	344	52	240	10	NF
122	2008	4	19	21:41:10.9	17.47	39.13	16.0	107	42	−39	3.6	Mw	CAP	Wf Inv	92	55	343	13	NF
123	2008	5	1	21:05:49.0	15.07	37.80	2.0	97	76	−2	2.8	Mw	CAP-PEPI	Wf Inv	53	11	321	8	SS
124	2008	5	13	21:28:30.0	15.06	37.80	12.0	76	46	−20	3.5	Mw	CAP-PEPI	Wf Inv	49	42	302	18	NS
125	2008	7	3	20:56:52.0	13.71	38.45	24.2	182	68	27	3.3	Mw	TDMT	Wf Inv	311	2	42	34	SS
126	2008	7	5	17:04:36.0	15.87	38.20	2.0	311	59	2	2.6	Mw	CAP-PEPI	Wf Inv	113	42	332	41	U
127	2008	8	15	01:45	16.09	40.54	32	290	75	−140	1.7	Ml	Frepoli&Al	Pol	156	38	54	15	SS
128	2008	9	1	14:45:40.0	15.06	37.97	8.1	70	31	−80	3.1	Mw	CAP-PEPI	Wf Inv	132	75	333	14	NF
129	2008	9	2	09:16:45.0	15.06	37.99	10.3	279	64	−44	3.3	Mw	CAP-PEPI	Wf Inv	239	49	338	8	NS
130	2008	9	27	8:28:27.17	17.22	39.19	10.0	222	85	14	3.6	Ml	TDMT	Wf Inv	356	6	87	13	SS
131	2008	10	27	10:55:55.0	15.13	38.11	2.0	50	28	−71	3.5	Mw	CAP-PEPI	Wf Inv	98	70	306	18	NF
132	2008	11	8	09:24	15.56	40.59	12.08	20	30	0	2.8	Ml	Frepoli&Al	Pol	353	38	227	38	U
133	2008	11	12	19:31	15.86	40.56	14.42	145	45	−60	2.4	Ml	Frepoli&Al	Pol	134	69	34	4	NF
134	2008	11	14	01:59	15.86	40.56	14.13	160	40	−80	2.8	Ml	Frepoli&Al	Pol	193	81	63	5	NF
135	2008	11	14	20:44	15.81	40.67	20.68	10	75	10	2.9	Ml	Frepoli&Al	Pol	324	4	233	18	SS
136	2008	11	17	00:13	15.85	40.56	16.94	165	20	−60	2.9	Ml	Frepoli&Al	Pol	208	61	52	27	NF
137	2008	11	18	19:54	15.84	40.56	15.7	135	60	−20	2.5	Ml	Frepoli&Al	Pol	99	34	3	8	SS
138	2008	11	18	20:05	15.84	40.56	15.97	75	50	−100	2.9	Ml	Frepoli&Al	Pol	292	81	172	5	NF
139	2008	11	18	22:14	15.85	40.55	16.51	175	75	−10	2.4	Ml	Frepoli&Al	Pol	132	18	41	4	SS
140	2008	11	20	14:09:19.0	17.49	39.14	15.0	166	82	−2	4.0	Mb	ItCMT	Wf Inv	121	7	31	4	SS
141	2008	11	27	23:49	15.86	40.55	12.94	130	65	−80	2.2	Ml	Frepoli&Al	Pol	60	68	213	19	NF
142	2008	11	28	23:39:21.0	13.69	37.54	35.0	337	74	9	4.2	Mb	ItCMT	Wf Inv	292	5	200	18	SS
143	2009	3	19	08:27:54.0	12.72	36.52	28.0	255	48	−180	4.0	Mb	ItCMT	Wf Inv	112	28	218	28	U
144	2009	4	27	09:42:15.7	15.08	38.07	30.0	69	78	−19	3.6	Mw	CAP	Wf Inv	25	22	117	4	SS
145	2009	7	1	17:58:54.1	15.01	38.34	2.0	40	90	19	3.1	Mw	CAP	Wf Inv	173	13	267	13	SS
146	2009	9	7	21:26:31.0	14.02	38.59	10.0	91	59	100	4.9	Mb	ItCMT	Wf Inv	174	13	27	74	TF
147	2009	11	8	06:51:16.0	14.55	37.83	15.0	310	21	−54	4.2	Mw	ItCMT	Wf Inv	344	60	192	27	NF
148	2009	12	19	09:01:18.9	15.09	37.76	40.0	112	44	176	4.6	Mw	ItCMT	Wf Inv	334	30	82	28	U
149	2010	2	8	07:23:57.8	16.77	39.49	34.0	94	73	−31	3.6	Mw	CAP	Wf Inv	51	34	146	8	SS
150	2010	3	17	11:01:11.4	14.73	38.57	8.0	78	56	81	3.3	Mw	CAP	Wf Inv	174	11	319	77	TF
151	2010	4	2	20:04:47.0	15.11	37.76	2.0	274	55	10	4.2	Mb	ItCMT	Wf Inv	231	21	329	21	U
152	2010	4	4	15:40:27.9	16.81	39.34	22.0	314	76	−18	3.3	Mw	CAP	Wf Inv	271	23	2	2	SS

(continued on next page)

Table 1 (*continued*)

ID	Year	Mn	Day	O.T.	Lon	Lat	Depth	Strike	Dip	Rake	Mag	M-Type	Source	Method	P_az	P_pl	T_az	T_pl	FT
153	2010	4	13	12:12:14.3	17.14	39.34	18.0	128	29	−26	3.5	Mw	CAP	Wf Inv	122	50	352	28	U
154	2010	4	15	20:05:47.1	17.21	39.35	18.0	137	39	−15	3.6	Mw	CAP	Wf Inv	113	42	356	26	U
155	2010	6	6	16:49:53.0	15.11	38.27	10.0	237	82	−34	3.5	Mw	CAP	Wf Inv	189	29	289	17	SS
156	2010	6	16	22:39:41.0	16.14	38.83	15.0	109	50	−38	4.1	Mw	ItCMT	Wf Inv	119	67	346	16	NF
157	2010	8	1	21:31:53.0	14.46	38.61	4.0	37	60	78	3.1	Mw	CAP	Wf Inv	136	14	278	72	TF
158	2010	8	16	12:54:46.0	14.92	38.42	10.0	218	66	42	4.5	Mw	CAP	Wf Inv	340	8	79	46	TS
159	2010	10	15	05:21:19.0	16.66	38.87	15.0	287	62	173	4.4	Mw	ItCMT	Wf Inv	57	8	148	4	SS
160	2011	5	6	15:12:35.0	14.96	37.78	22.2	13	57	15	4.0	Mb	ItCMT	Wf Inv	328	13	229	33	SS
161	2011	6	23	22:02:46.0	14.76	38.06	7.4	59	44	−130	4.1	Mb	ItCMT	Wf Inv	252	62	356	8	NF
162	2011	7	6	09:08:38.0	14.80	38.01	7.5	115	44	−53	3.7	Mb	ItCMT	Wf Inv	104	64	360	7	NF
163	2011	11	15	04:59:00.0	14.67	38.25	7.0	281	80	66	4.0	Ml	TDMT	Wf Inv	31	31	165	49	U
164	2011	11	23	14:12:33.0	16.02	39.92	6.3	319	51	−106	3.6	Ml	TDMT	Wf Inv	171	77	60	5	NF

Database of 164 selected earthquake focal mechanisms for the Calabrian Arc. ID is the order number (see same label numbers in Fig. 4). Strike, dip, and rake refer to the nodal planes. Mag is the earthquake magnitude with the specific scale (M-Type). Source is the bibliographic source: Italian Centroid Moment Tensor (ItCMT); Time-Domain Moment Tensor (TDMT); D'Amico et al. (2011) (CAP-BGTA); D'Amico et al. (2010) (CAP-PEPI); Maggi et al. (2009) (Maggi&Al); Li et al. (2007) (CAP-BSSA); Frepoli et al. (2011) (Frepoli&Al); CAP denotes 17 new mechanisms computed with the CAP method. Method is the methodology applied to compute the mechanisms: Waveform inversion (Wf Inv) and P-onset polarity analyses (Pol). P_Az and T_Az mean azimuth of P- and T-axes, respectively. P_Pl and T_Pl mean plunge of P- and T-axes, respectively. FT is faulting type according to Zoback's (1992) definition: NF = normal faulting, NS = normal faulting with a minor strike-slip component, SS = strike-slip faulting, TF = thrust faulting, TS = thrust faulting with a minor strike-slip component, and U = unknown stress regime.

2008, 2011; Devoti et al., 2008, 2011; Hollenstein et al., 2003; Palano et al., 2011, 2012; Serpelloni et al., 2007, 2010) with a marked kinematic divergence between Calabria and Sicily and active shortening in the Ionian section of the Calabrian Arc and in the south-Tyrrhenian. Several sectors of the Calabrian Arc and adjacent areas are seismically active as demonstrated by recent and historical earthquakes (Basili et al., 2008; Chiarabba et al., 2005; Galli et al., 2008). The main known seismic faults or zones in the Calabrian Arc and adjacent areas are synthetically depicted as follows from northeast to southwest (Fig. 1a).

(1) The inner (Tyrrhenian) and axial sectors of Southern Apennines have undergone postorogenic extensional tectonics since at least early-middle Pleistocene time (Amicucci et al., 2008; Barchi et al., 2007). Although several destructive earthquakes in recent and historical times were sourced by normal faults in the axial and inner Southern Apennines (Galli et al., 2006, 2008; Pantosti et al., 1993), most seismically active faults of this region are still poorly known. Recently, Brozzetti (2011) has integrated the long literature on the neotectonics of Southern Apennines (e.g., Ascione et al., 2003; Boncio et al., 2007; Cinque et al., 1993; Frepoli et al., 2005, 2011; Galli and Galadini, 2003; Giano et al., 2000; Improta et al., 2010; Maschio et al., 2005; Moro et al., 2007; Pantosti and Valensise, 1990; Papanikolaou and Roberts, 2007; Spina et al., 2008; Valoroso et al., 2009, 2011; Villani and Pierdominici, 2010; Westaway and Jackson, 1984) with new data and has recognized an extensional belt including three main fault alignments trending NW–SE. Each alignment consists of normal fault segments up to about 25 km in length and to a few kilometers in cumulated displacement. Slip on these faults is in general compatible with a NE–SW extension, but strike-slip seismic sequences have also been recorded such as the 1990–1991 Potenza sequence that occurred along a N100°-trending fault zone (Boncio et al., 2007).

(2) The Ionian side of northern Calabria (off northeastern Sila) is a tectonically complex area as it joins the NW–SE-trending, NE–SW-extending Southern Apennines with the NNE–SSW-trending, NW–SE-extending curved Calabria, and it is located on top of the northern edge of the subducting Ionian slab (Fig. 1c). The Ionian side of northern Calabria (including the northeastern Sila Massif, the Sibari Plain, and the eastern Pollino Range) is a seismically active area, where some historical and recent earthquakes were recorded (Arrigo et al., 2006; Galli and Scionti, 2006). Moreover, in this area, geomorphologic, structural, and offshore reflection seismic evidence has revealed the presence of active NW-striking transpressional faults that may accommodate a large part of the geodetic shortening shown by GPS data between the Southern Apennines and the Apulian foreland toward the northeast (Cinque et al., 1993; Del Ben et al., 2008; Ferranti et al., 2009; Spina et al., 2009). Seismic reflection data suggest a recent transpressional activity along the NW-striking faults of this area (Sibari strike-slip fault in Del Ben et al., 2008). The active tectonics, kinematics, and recent deformation rates of this area remain, however, largely debated as demonstrated in several studies (Cinti et al., 1997; Cucci, 2004; Del Ben et al., 2008; Galadini et al., 2000; Molin et al., 2004; Tansi et al., 2007). Paleoseismological evidence of a left-lateral activity has been also found to the south of the Sibari Plain, namely along the NW-striking Cecita and Lake faults that cut across the Sila Massif (Galli and Bosi, 2002).

(3) Calabria is a curved region hosting the central and most curved portion of the Calabrian Arc. This region tops the narrow Ionian slab subducting toward the northwest (Fig. 1c) and it is mostly undergoing active extension (D'Agostino et al., 2011). Two main systems of active normal faults are present in Calabria. Toward the northwest (Tyrrhenian side of Calabria), the system of the Crati River (Cello et al., 1982; Cifelli et al., 2007; Spina et al., 2009, 2011; Tortorici et al., 1995a) includes N-striking normal faults with some evidence of recent oblique dextral motions along the boundaries of the narrow Crati River basin. Recent intermediate-magnitude extensional earthquakes that occurred in 1980 (M 4.3) and 2001 (M 4.2) as well as the 1638 destructive earthquake (M c. 6.7) prove the ongoing activity of the Crati River fault system. Toward the south, along the Tyrrhenian side of Calabria, the Serre–Cittanova system (Galli and Bosi, 2002; Jacques et al., 2001; Monaco and Tortorici, 2000; Tortorici et al., 1995a) includes active normal faults striking NE–SW and separating the Aspromonte and Le Serre ranges, to the east, from a series of basins occurring along the Tyrrhenian side of Calabria. This fault system and other nearby faults have been involved in destructive historical earthquakes and earthquake sequences that occurred in 1783, 1894, 1905, 1907, and 1908 (Galli and Bosi, 2002; Neri et al., 2006), which involved a large part of Calabria down to the Messina Straits.

(4) Between Calabria and Sicily, the Messina Straits is one of the most enigmatic areas of the entire Calabrian Arc (Doglioni et al., 2012). On December 1908, a magnitude 7.1 earthquake and subsequent tsunami (Billi et al., 2008, 2009b, 2010a; Pino et al., 2009) provoked tens of thousands of deaths and enormous damage to the cities and villages along the straits. The 1908 earthquake may have been caused by the activation of a normal, circa north–south trending fault in the Messina

Straits responding to the general WNW–ESE active extension detected by seismological and GPS data (Neri et al., 2005; Serpelloni et al., 2010); however, the exact location and geometry of the 1908 earthquake-causative fault are still controversial (Amoruso et al., 2002, 2006; Boschi et al., 1989; Bottari et al., 1989; Catalano et al., 2008; DISS Working Group, 2007; Monaco and Tortorici, 2000; Pino et al., 2009; Valensise and Pantosti, 1992), whereas both recent and past studies have made clear that the destructive tsunami associated to this earthquake was sourced, for its largest part, by an underwater landslide located to the south of the main epicentral area (Billi et al., 2008, 2009a; Ryan and Heezen, 1965). The seismicity in the Messina Straits in the last few decades (Neri et al., 2003, 2004, 2008) has not allowed seismologists to accurately define the locations and mechanisms of the seismogenic faults in this area. Recently, Polonia et al. (2011, 2012), through offshore seismic reflection investigations, have drawn a long, segmented, NW–SE deformation zone running from the Messina Straits toward the southeast and accommodating active differential movements of the Calabrian and the Peloritan portions of the Calabrian Arc.

(5) To the south of the Messina Straits, off eastern Sicily, the Malta escarpment is another enigmatic morphostructural feature. This feature, which runs NNW–SSE from the Maltese Islands, to the south, to almost Mt Etna, to the north, is primarily a morphological escarpment separating the Hyblean–Pelagian continental domain, to the west, from the low-altitude presumably-oceanic Ionian domain, to the east (Grasso, 1993). Recent studies have shown that the southern portion of this feature is tectonically inactive, whereas evidence of active tectonics is present along some fault segments accompanying the escarpment in its northern section (Polonia et al., 2011, 2012). The inactivity of part of the Malta escarpment as well as the hypothesized landslide source for the tsunami that followed the 1693 magnitude 7.3 destructive earthquake of southeastern Sicily (Billi et al., 2010b) may support the hypothesis that the causative fault of this strong earthquake is inland along active faults that cut through the Hyblean foreland in southeastern Sicily (e.g., Bianca et al., 1999; Sirovich and Pettenati, 2001; Visini et al., 2009). The offshore hypothesis remains, however, also plausible (e.g., Gutscher et al., 2006).

(6) To the west of the Messina Straits, the Tindari Fault system (including some active Aeolian volcanoes) constitutes a complex right-lateral transtensional active zone (NNW-trending) of seismic deformation (Billi et al., 2006; Goes et al., 2004; Pondrelli et al., 2004a; Tortorici et al., 1995b). Toward the north, the offshore and coastal sections of the Tindari Fault are sites of frequent low- and intermediate-magnitude earthquakes (Billi et al., 2006). Toward the south, this fault system becomes less definite and probably spread over a diffuse zone of brittle deformation close to Mt Etna, beneath which NW-striking right-lateral seismic faulting is particularly frequent with low- and intermediate-magnitude earthquakes (Aloisi et al., 2002; Barberi et al., 2000; Cocina et al., 1997, 1998; Gresta et al., 2005). The Tindari Fault system and the active right-lateral strike-slip faulting in northeastern Sicily are interpreted by many as a diffuse regional transfer zone between the compressional south-Tyrrhenian domain and the extensional Ionian one (Billi et al., 2006; Goes et al., 2004; Govers and Wortel, 2005; Pondrelli et al., 2004a). The Tindari Fault system is located on top of the southern edge of the Ionian subducting slab and, as such, is considered as a possible expression of a subduction-transform edge propagator or STEP fault (Govers and Wortel, 2005; see also Rosenbaum et al., 2008) on the overriding plate.

(7) To the west and northwest of Mt Etna, a roughly WNW-trending zone of seismic deformation runs between Mt Etna and Cefalù along the northern coast of Sicily (Billi et al., 2010b). This zone includes disconnected, short (up to 15–20 km in length), normal fault segments preferentially striking WNW–ESE, but, in places, abutted by N- to NNE-striking strike-slip faults. The overall kinematics of the Cefalù–Etna zone is extensional (NNE–SSW extension; Hollenstein et al., 2003; Billi et al., 2010b) and becomes right-lateral transtensional toward the east close to Mt Etna. On the basis of historical data and apparent fault size, the maximum expected earthquake magnitude for the Cefalù–Etna seismic zone results to be of class 6 (Billi et al., 2010b; see also Barreca et al., 2010) but wider investigations are required for a more effective evaluation of the seismic potential in this area. The geodynamic engine activating this extensional zone located within the broader convergent boundary between Europe and Africa (Nubia) is still substantially unknown. Lateral extension on preexisting faults and upwelling of melt mantle material beneath Mt Etna were considered viable processes to explain, at least in part, the active extensional tectonics along the Cefalù–Etna seismic zone (Billi et al., 2010b).

(8) To the north of Sicily, a compressional belt of seismic deformation runs approximately E–W in the south-Tyrrhenian from the Tindari Fault, to the east, toward Ustica Island, to the west (Billi et al., 2007, 2011; Cuffaro et al., 2011; Goes et al., 2004; Montone et al., 2004; Pondrelli et al., 2004a; Presti et al., 2008). This belt includes fault segments that strike NE–SW and NW–SE. Earthquake data show that the NE-striking faults are mainly reverse, whereas the NW-striking ones are mainly right-lateral strike-slip or transpressional. Several historical earthquakes that caused damage in Palermo and in other inhabited sites of northern Sicily are thought to be sourced from the compressional belt of southern Tyrrhenian rather than from local inland sources (Azzaro et al., 2004; Guidoboni et al., 2003). On the basis of historical data and apparent fault size, the maximum expected earthquake magnitude for this seismic belt results to be of class 6, but larger events cannot, at the present level of knowledge, be excluded (Billi et al., 2007). Most seismically-active faults in the south-Tyrrhenian belt are high-angle. For this reason and for seismic reflection evidence, it is plausible that the seismicity in this sector is due to a reactivation (rejuvenation) of the inner Calabrian orogenic wedge (Billi et al., 2007; Pepe et al., 2005). The compressional south-Tyrrhenian belt may become, in the future, a new convergent plate boundary with southward subduction of the Tyrrhenian backarc basin (Billi et al., 2011).

(9) Compression in central Sicily and in the Sicily Channel is considered substantially inactive since Pleistocene–Holocene times by several investigators (e.g., Butler and Grasso, 1993). However, on January 1968, a magnitude 5.6 earthquake, accompanied by two other M 5.2 shocks hit the Belice Valley in central-western Sicily. Instrumental records of this mainshock are limited and led to the elaboration of two main types of focal mechanisms: one strike-slip (Anderson and Jackson, 1987) and one compressional (Monaco et al., 1996). Another compressional earthquake (M 4.9) occurred on June 1981 to the west of Belice Valley, close to Mazara del Vallo (Lavecchia et al., 2007b; Pondrelli et al., 2004a). The Belice Valley is presently affected by infrequent low-magnitude seismicity. The above mentioned seismic evidence suggests that some contractional deformation is still being accommodated in central-western Sicily (Speranza et al., 1999; Lavecchia et al., 2007a, 2007b; see also GPS evidence in Billi et al., 2011). By use of several types of seismic, geophysical, and geological data, some investigators (Lavecchia et al., 2007b; Sgroi et al., 2012; Visini et al., 2010) suggested the existence of a unique regional-scale seismogenic structure (Sicilian Basal Thrust) connecting the active deformation and the seismic activity of the western, central and eastern areas of mainland Sicily and those of central-southern Sicily, subject to a NNW-striking compressional stress regime.

2.2. Lithosphere and mantle structure

The lithosphere and mantle setting beneath the Calabrian Arc has been deeply investigated in the last decades by means of regional and local seismic analyses reported in several previous papers (Barberi et al., 2004; Chiarabba et al., 2008; Chironi et al., 2000; Montuori et al., 2007; Neri et al., 2002; Steckler et al., 2008). Although very heterogeneous, the Calabrian Arc is characterized by a set of well determined first-order crustal and sub-crustal features, which are well visible in Fig. 2. This figure synthesizes the most recent P-wave velocity models available for the study area (Neri et al., 2009; Orecchio et al., 2011). At a depth of 10 km (Fig. 2a), different velocity patterns are evident for the Tyrrhenian Sea, Sicily, Calabria, and Southern Apennines. Sicily and Southern Apennines are characterized by P-wave velocity values of about 5–5.5 km/s, which are typical of continental crusts, whereas, beneath Calabria and the Tyrrhenian Sea, the tomographic analysis reveals higher P-wave velocities (c. 6–6.5 km/s). The high velocity pattern beneath the Tyrrhenian Sea is commonly interpreted with the thinning of the Tyrrhenian crust (and incipient oceanization) with respect to the adjacent continental crusts of Sicily and Southern Apennines (Barberi et al., 2004; Chiarabba et al., 2008; Finetti, 2005a, 2005b; Orecchio et al., 2011; Pepe et al., 2000). The high-velocity pattern beneath Calabria (at a depth of 10 km), contrasting with slower ones at the same depth beneath Southern Apennines and Sicily, shows lateral heterogeneities in the roots of the large Calabrian Arc (see also Di Stefano et al., 2009; Piana Agostinetti and Amato, 2009). In short, the velocity map at 10 km depth (Fig. 2a) provides evidence for the crustal heterogeneities and boundaries between the main crustal domains of Calabro–Tyrrhenian, Sicilian, and Southern Apennines regions.

At 30 km of depth (Fig. 2b), we identify a high velocity domain beneath Tyrrhenian Sea, which is interpreted as a mantle domain, and a more uniform domain beneath the Calabrian Arc, which is interpreted as a lower-crust domain (Barberi et al., 2004, Chiarabba et al., 2008; Finetti, 2005a, 2005b; Orecchio et al., 2011). The different velocity domains beneath Calabria and Tyrrhenian Sea as well as the rather homogeneous pattern beneath the Calabrian Arc are interpreted with a crustal thickening beneath the arc (i.e., the accretionary wedge; Barberi et al., 2004; Catalano et al., 2001; Finetti, 2005a, 2005b). In particular, the P-wave velocity values (c. 6.5–7 km/s) obtained below the arc may correspond either to continental lower-crust rocks of Sicily and Southern Apennines or to crustal rocks of the Ionian slab subducting toward the northwest beneath the Calabrian Arc (Fig. 2e and f).

The NNW-trending high-velocity anomaly reported at 65 km of depth (Fig. 2c) identifies the subducting Ionian lithosphere approaching the flexure zone located beneath the Tyrrhenian coast of Calabria. Locations of the low velocity anomalies are compatible with toroidal circulations of asthenospheric material around the narrow slab (Fig. 1c) as suggested by previous papers (Civello and Margheriti, 2004; Faccenna et al., 2005, 2011; Lucente et al., 2006; Montuori et al., 2007; Piromallo et al., 2006). The Ionian lithospheric slab has its shortest along-strike extent at 105 km depth, where the high velocity anomaly is present only beneath southern Calabria along a NE-striking c. 100 km-long segment. This tomographic result suggests that the subducting lithosphere is presently continuous only beneath southern Calabria (i.e., the central portion of the Calabrian Arc), whereas slab break-off has already occurred at the northern and southwestern edges of the arc (i.e., beneath northern Calabria and northeastern Sicily, respectively). To better illustrate the subduction setting, in Fig. 2(e) and (f), we show two vertical cross-sections, one orthogonal and one parallel to the Ionian slab. The AA′ cross-section (Fig. 2e) tidily shows the depth continuity of the Ionian slab beneath southern Calabria as well as the crustal tectonic doubling beneath Calabria. In the BB′ cross-section (Fig. 2f), the lateral boundaries of the narrow Ionian slab are well evident as it is also the crustal thinning of the Tyrrhenian crust with respect to the adjacent crusts of Sicily and Southern Apennines.

3. Earthquake focal mechanisms

3.1. Method and data selection

To constrain the active tectonics and seismogenic stress fields of the Calabrian Arc region, we compiled an up-to-date database (Table 1) including all the available crustal focal mechanisms computed for the study region by using waveform inversion methods (http://www.bo.ingv.it/RCMT/; http://cnt.rm.ingv.it/tdmt.html; Li et al., 2007; D'Amico et al., 2010, 2011) and some well constrained first-motion focal mechanisms (Frepoli et al., 2011, Maggi et al., 2009). In the database, we also included seventeen new focal mechanisms computed through the CAP waveform inversion method.

In constraining focal mechanisms, waveform modeling is well known to be a much more powerful method than first-motion inversion. First-motion focal solutions strongly suffer from the uncertainties on velocity models required to reconstruct the wave path, reflect only the initial stages of faulting, and may be unstable due to a poor azimuthal coverage of the observing stations (Lay and Wallace, 1995; Pondrelli et al., 2006; Scognamiglio et al., 2009). In particular, in the study region, the seismic network geometry affected by the lack of OBSs (Ocean Bottom Seismometers) in the wide offshore region (Fig. 1b) is a major factor reducing the quality of traditional focal mechanisms obtained from the inversion of P-onset polarities (D'Amico et al., 2010; Pondrelli et al., 2006). For this reason, although the first-motion focal mechanisms in the study region display focal parameter errors small enough to allow detection of gross variations of stress (e.g., between the Calabrian Arc and western-central Sicily major domains; Frepoli and Amato, 2000a), their uncertainties are too large for detection of slighter stress changes of our interest in the present study. All these considerations led us to compile a database of selected focal mechanisms (Table 1) by principally using waveform inversion solutions, but including also a few high-quality data resulting from quality-selected P-onset polarity inversions.

As regards moment tensor solutions, in our database (Table 1), most data are from the Italian CMT catalog (ItCMT, 79 events) covering the time interval 1977–2011. For the period 2004–2011, the database includes also focal solutions computed by using the Time-Domain Moment Tensor (TDMT, 10 events), and the Cut and Paste technique (CAP, 53 events).

The Italian CMT catalog (http://www.bo.ingv.it/RCMT/Italydataset.html; Pondrelli et al., 2006) has been obtained by merging the existing global CMTs, the Euro-Mediterranean RCMTs, and the solutions computed to extend backward the Euro-Mediterranean RCMT catalog. This catalog represents an extension toward smaller magnitudes of the Harvard Centroid Moment Tensor catalog (CMT). The CMT database furnishes robust, stable, and reliable seismic source mechanisms through the analysis of intermediate and long period seismograms recorded at the global scale for earthquakes with $M > 5$ (Dziewonski et al., 1981; Ekström et al., 2005). This inversion process simultaneously fits two signals: (1) the very long period ($T > 40$ s) body wave train from the P-wave arrival until the onset of the fundamental modes and (2) the mantle waves ($T > 135$ s). Moment tensors for $4.0 \leq M \leq 5.5$ earthquakes in the Italian CMT catalog have been computed following

Fig. 2. Crustal and sub-crustal P-wave velocity models selected from recent tomographic analyses (Neri et al., 2009; Orecchio et al., 2011). (a) and (b) show the crustal velocity model obtained by Orecchio et al. (2011) at depths of 10 and 30 km, respectively. (c) and (d) show the subcrustal results of Neri et al. (2009) at depths of 65 and 105 km in terms of percentage velocity variation with respect to the ak135 model. Numbers in low-right corners indicate depths in kilometers below sea level. Black curves contour the good resolution zones as reported in the original works (Neri et al., 2009; Orecchio et al., 2011). (e) and (f) show two cross-sectional views perpendicular and parallel, respectively, to the Calabrian Arc (see cross-section tracks in Fig. 2a). Data are from Orecchio et al. (2011) for depths between 0 and 50 km, and from Neri et al. (2009) for depths greater than 65 km.

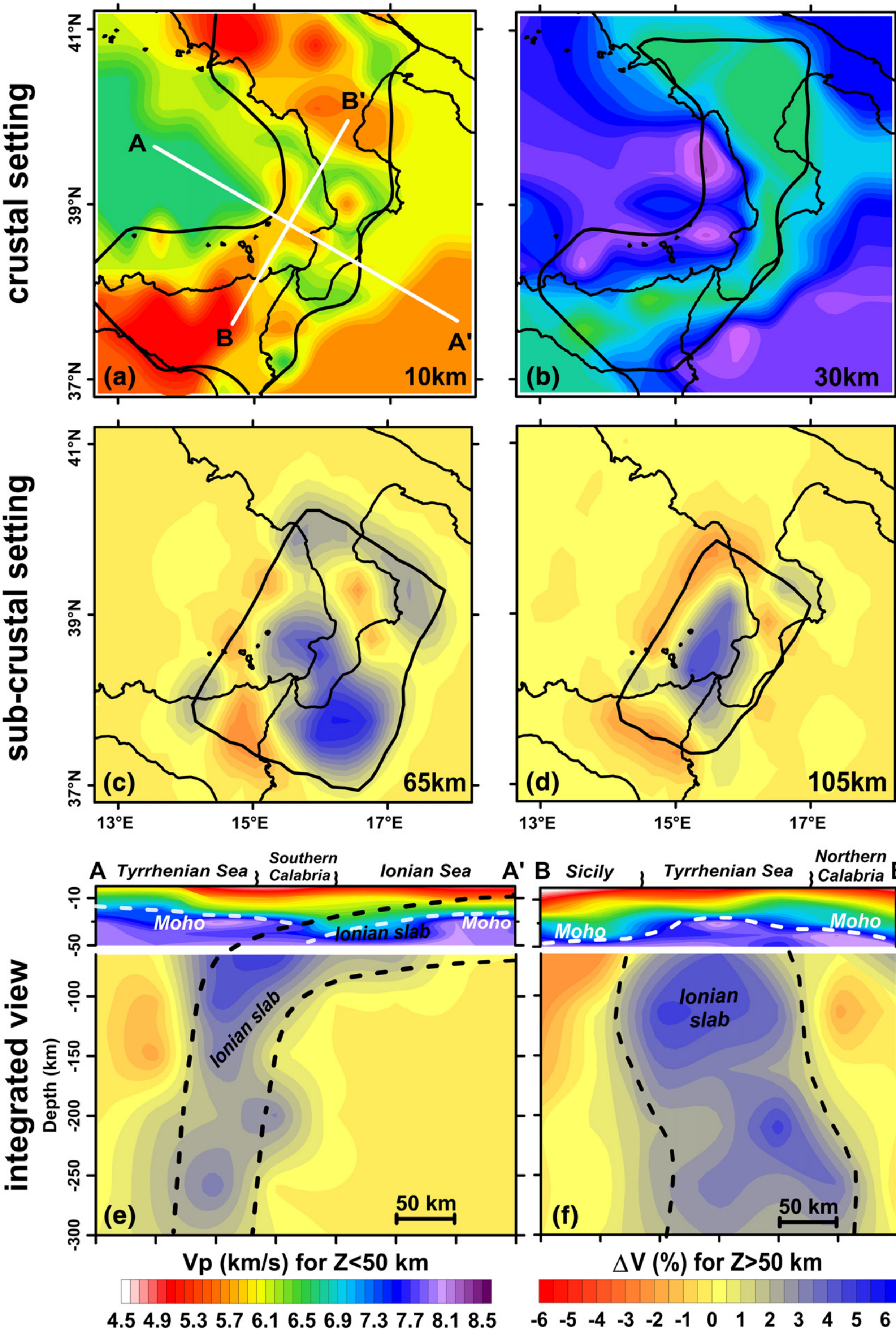
crustal setting
sub-crustal setting
integrated view
(a) 10km
(b) 30km
(c) 65km
(d) 105km
A
A'
B
B'
41°N
39°N
37°N
13°E
15°E
17°E
A Tyrrhenian Sea Southern Calabria Ionian Sea A'
B Sicily Tyrrhenian Sea Northern Calabria B'
Moho
Ionian slab
Ionian slab
Depth (km)
-10
-30
-50
-100
-150
-200
-250
-300
(e)
(f)
50 km
50 km
Vp (km/s) for Z<50 km
4.5 4.9 5.3 5.7 6.1 6.5 6.9 7.3 7.7 8.1 8.5
ΔV (%) for Z>50 km
-6 -5 -4 -3 -2 -1 0 1 2 3 4 5 6

the same method that is used to analyze current seismicity for the European-Mediterranean RCMT Catalog (http://www.bo.ingv.it/RCMT/). The RCMT procedure is based on the inversion of intermediate and long period surface waves recorded at regional and teleseismic distances. Observed and synthetic seismograms are matched after a low-pass filtering with a cutoff period generally set at 35 s. The quality evaluation process included in this procedure ensures a high reliability of data (Pondrelli et al., 2002, 2004b, 2006, 2007, 2011).

The TDMT algorithm performs long-period full waveform inversion for local and regional events with magnitude M≥3.5 (Dreger, 2003; Dreger and Helmberger, 1993; Scognamiglio et al., 2009; http://earthquake.rm.ingv.it/tdmt.php). Waveforms are corrected for the instrument response, integrated to obtain displacement, and then band-pass filtered in the frequency band 0.02–0.05 Hz, for events with $M_L \geq 3.8$, and in the band 0.02–0.1 Hz, for events with magnitude smaller than 3.8. Focal mechanisms judged not reliable according to a quality index scale based both on the number of stations used and on the double-couple value are not included in the dedicated web site (Scognamiglio et al., 2009) and therefore also in our database.

In the CAP method (Zhao and Helmberger, 1994; Zhu and Helmberger, 1996), each waveform is broken up into Pnl (i.e., the first arrivals from a seismic source located in the crust eventually including waves reflected and multireflected from the top of the sharpest discontinuity) and surface wave segments, which are weighted differently during the inversion procedure. This procedure is necessary because the selected wave segments are sensitive to different parts of crustal structure and have different amplitude decay with distances. The surface waves, although large in amplitudes, are easily influenced by shallow crustal heterogeneities, whereas Pnl waves are controlled by the averaged crustal velocity structure and are therefore more stable. Ground velocity data are preferred to ground displacement mainly because of the use of weak-motion data and because, for earthquakes of magnitude less than 4, there is a high signal-to-noise ratio only at higher frequencies. Furthermore, working with ground velocity rather than ground displacement reduces the influence of a low frequency site or instrument noise on the deconvolution. Synthetic and observed ground velocities are filtered in the same frequency bands, namely from 0.02 to 0.1 Hz, for the surface waves, and from 0.05 to 0.3 Hz, for the Pnl waves. All these features make the CAP method effective for earthquakes over a wide range of magnitudes (down to a minimum of 2.6; D'Amico et al., 2010, 2011; Zhu et al., 2006) as also proven by several tests and comparisons (D'Amico et al., 2010, 2011, Tan et al., 2006, Zhao and Helmberger, 1994). The stability of previously-published CAP mechanisms was accurately verified by varying both the Earth structure parameters and the recording network distribution (D'Amico et al., 2010, 2011). The fault parameter uncertainties were estimated in D'Amico et al. (2010) as lower than 6° using the methods and the statistical approaches described by Tan et al. (2006) and Bevington and Robinson (2003).

For this work, we elaborated 17 new focal mechanisms (highlighted in Fig. 4 with a thicker perimeter) using the CAP method for earthquakes that occurred between 2005 and 2010 (magnitude range 3.1–4.5) and successfully tested the stability of these new data. As explicatory examples, in Fig. 3, we show the stability tests for two of our new CAP focal mechanisms selected in order to check the method at the lowest and highest earthquake magnitudes of the dataset. In particular, Fig. 3 shows the stability of the focal mechanism solutions in different seismic network conditions (plots (a) and (b)) and in the neighborhood of the estimated focal depth (plot (c)).

For 24 earthquakes that occurred between 2004 and 2010, different solutions are reported in the different catalogs. In these cases, we made our choice selecting the final focal mechanism to be included in Table 1 according to the following order of preference: CAP, ItCMT, and TDMT. As the tests performed by Scognamiglio et al. (2009) showed a good agreement between the TDMT and ItCMT catalogs, we preferred the solutions coming from the richer ItCMT catalog to ensure a better continuity over the whole database. Following D'Amico et al. (2011), we also verified for the solutions estimated in the present study the agreement between the CAP, TDMT and ItCMT solutions by means of the Kagan angles (Kagan, 1991). These angles measure the rotation that must be applied to a double-couple source to make it coincident with another one. The Kagan angles can vary from 0° (indicating perfect agreement between the two solutions) to 120° (total disagreement). Values below 60° indicate a good agreement between the two solutions (Pondrelli et al., 2006). The Kagan angles estimated in D'Amico et al. (2011) and in the present study show a good correspondence between CAP and other solutions. For these events, the CAP solutions were preferred to the TDMT and ItCMT ones because the CAP solutions were computed using velocity models specific of the study region (instead of large-scale averaged models) and were also carefully checked for quality and stability by properly planned tests both in the studies by D'Amico et al. (2010, 2011) and in the present work (e.g., Fig. 3).

Concerning the first-motion focal mechanisms, the area under investigation in this paper includes some sectors (Southern Apennines and central Calabria) characterized by a good seismic station coverage (Fig. 1b) and for which focal mechanisms estimated by the first-motion method can also be well constrained. To select high-quality first-motion focal mechanisms from these sectors, we considered previously-published papers reporting polarity distribution on the focal sphere or, at least, polarity number and quality parameters of solutions (Frepoli and Amato, 2000a; Frepoli et al., 2011; Giampiccolo et al., 2008; Maggi et al., 2009; Vannucci and Gasperini, 2004). We then selected good quality focal mechanisms with a number of polarities larger than or equal to 14. This selection provided 22 very reliable first-motion focal mechanisms from the Southern Apennines. We therefore included these latter mechanisms in the database (Table 1).

3.2. Spatial distribution of focal mechanisms

All focal mechanisms included in our database (Table 1) are displayed in Fig. 4 with different colors corresponding to different types of faulting according to the Zoback's standard classification used in the World Stress Map and based on different plunge ranges for P- and T-axes (Zoback, 1992; http://dc-app3-14.gfz-potsdam.de/): Normal Faulting (NF), Normal Strike (NS), Strike-Slip (SS), Thrust-Strike (TS), Thrust Faulting (TF) and Unknown (mechanisms with P- and T-axes falling outside the ranges of the other categories). In Fig. 4, the NF and NS categories are grouped together (same color) as well as the TF and TS categories. Epicenters of earthquakes listed in Table 1 and displayed in Fig. 4 are shown in the map of Fig. 5 and are grouped by polygons according to a criterion of homogeneity based on visual inspection of focal mechanisms and of polar plot distributions of P- and T-axes. Although preliminary, this partitioning shows a certain correspondence with the main seismotectonic features of the study region described in Section 2.1. The depth distribution of the same earthquakes/mechanisms is shown in Fig. 6.

Normal faulting is predominant over most of the Calabrian Arc. In particular, from the Southern Apennines to Sicily, about 40% of the focal mechanisms from our database are normal or oblique-extensional. Reverse faulting is predominant in the southern Tyrrhenian area (Fig. 4), where the P-axes (horizontal, NW–SE-trending; Plot 1 in Fig. 5) are consistent with the NW–SE Nubia–Eurasia convergence (Billi et al. 2007, 2011; Neri et al., 2005; Pondrelli et al., 2004a). This same trend of P-axes (Plot 4 in Fig. 5) is also characteristic of focal mechanisms from the Hyblean–Pelagian foreland (Sicily Channel) south of latitude N37.5° (Fig. 4).

The central-northern Sicily between about Mt Etna and Cefalù is affected by NNE–SSW extension over a complex fault network striking WNW–ESE or N–S (Billi et al., 2010b). Strike-slip kinematics becomes predominant over northeastern Sicily and the Etnean area.

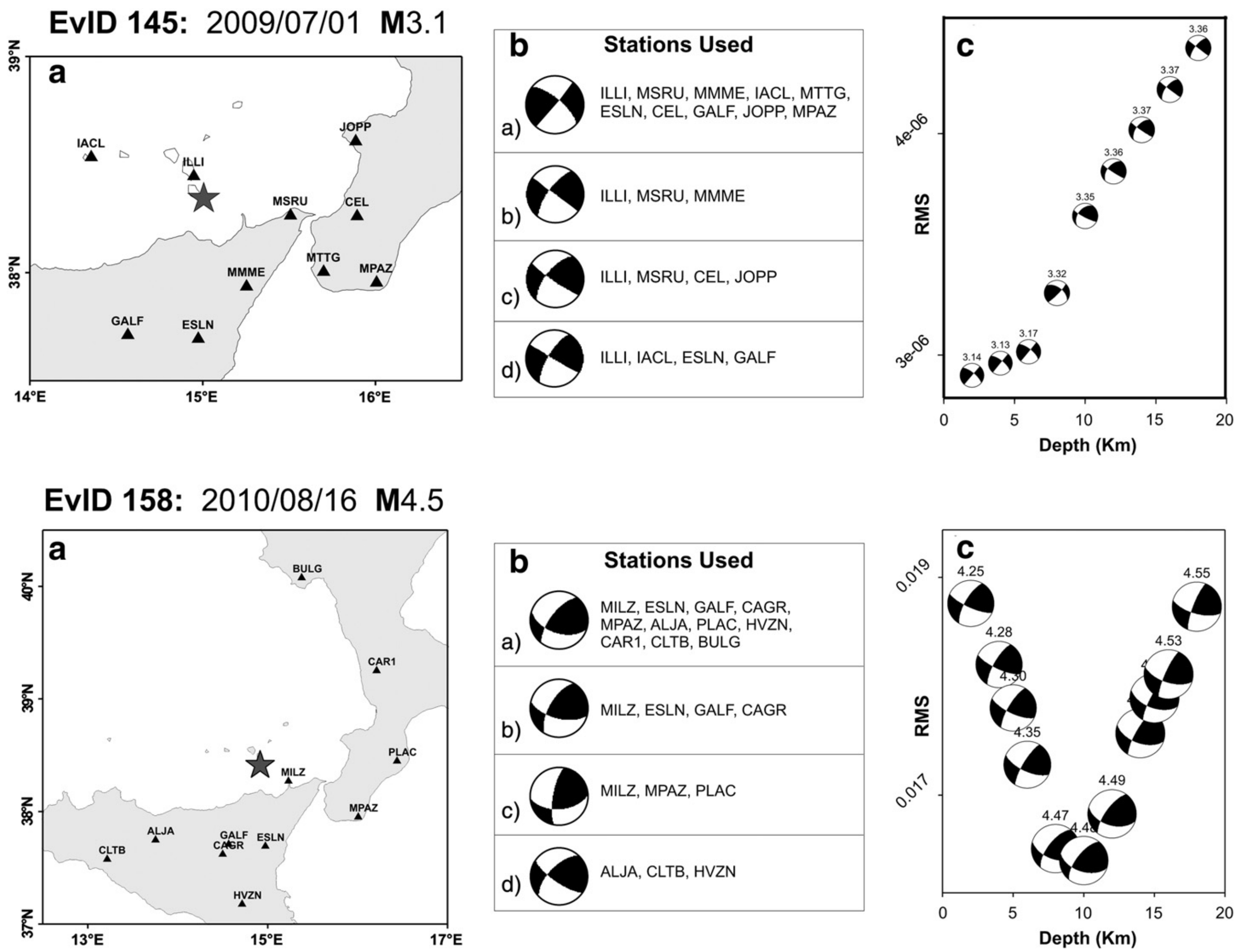

Fig. 3. Two examples of tests performed to verify the stability of the focal mechanisms estimated in this work (Table 1). (a) These two panels show the location of the events and stations used in the tests. (b) Beach balls represent the solutions obtained using different sets of stations. (c) Misfit errors reported as a function of depth. The solutions do not change around the minimum, thus indicating the stability of the final solution.

Along the Tindari Fault system, right-lateral to oblique-extensional displacements are presently accommodated (Plot 3 in Fig. 5), thus indicating this fault system as the possible junction along which the horizontal displacements, presently active in the south-Tyrrhenian belt, are transferred toward the southeast in the Ionian section of the Calabrian Arc (Billi et al., 2006; Goes et al., 2004). Toward the north, also the Ionian side of northern Calabria is characterized by (left-lateral) strike-slip seismic faulting along the NW–SE direction. Analogously to the Tindari Fault system, also the Ionian side of northern Calabria (i.e., northeast of Sila) may constitute a strike-slip transfer zone connecting the tectonically heterogeneous central Calabria and Southern Apennines.

The Etnean area is mainly affected by strike-slip seismic faulting, which becomes prevailing toward the east. In particular, the related P- and T-axes (Plot 5 in Fig. 5) suggest, for the Etnean area, prevailing right-lateral dislocations along WNW- and NW-striking faults. Both strike-slip, extensional, and reverse earthquakes occurred, however, in recent decades in the Etnean area, particularly during or immediately before important eruptive periods (e.g., Alparone et al., 2011; Barberi et al., 2000; Bonanno et al., 2011; Gresta and Patanè, 1987; Gresta et al., 2005; Neri et al., 2005; Patanè et al., 2003). We carefully verified in the present study that no earthquake of our dataset (Table 1) occurred during or close to the Etna's eruptive periods in the crustal volume that several investigators proposed as the most significantly affected by the local volcanic processes (see, e.g., Cocina et al., 1998; Barberi et al., 2000). This check, together with the additional support of the observed waveform features and of published information concerning earthquakes anyway located near the volcano edifice, allows us to be very confident that all the earthquakes listed in Table 1 had a tectonic origin. The right-lateral strike-slip regime suggests that similar seismic processes occurred in the Mt Etna domain and in the northern portion of the Tindari Fault system near the central Aeolian Islands. This evidence led us to display, in Fig. 5, also the joint polar plot "3 + 5" of P- and T-axes distributions. The coherency of the resulting joint distribution further indicates the homogeneous behavior of these two sectors thus supporting the presence of a diffuse transfer zone from Mt Etna to the central Aeolian Islands along the Tindari Fault system (Billi et al., 2006; Goes et al., 2004). Extension is dominant in the Central Calabria to Messina Straits area (see also D'Amico et al., 2010; Serpelloni et al., 2010), where most events have near vertical P-axes and circa horizontal T-axes trending WNW–ESE (Plot 6 in Fig. 5). The indentation of this extensional domain (CCMS for brevity) into the northeastern corner of Sicily – already suggested in the previous stress analysis of Neri et al. (2005) – is now further confirmed by the new, higher-quality data that clearly show the CCMS extensional volume to be wedged into the Northeastern Sicily strike-slip transfer

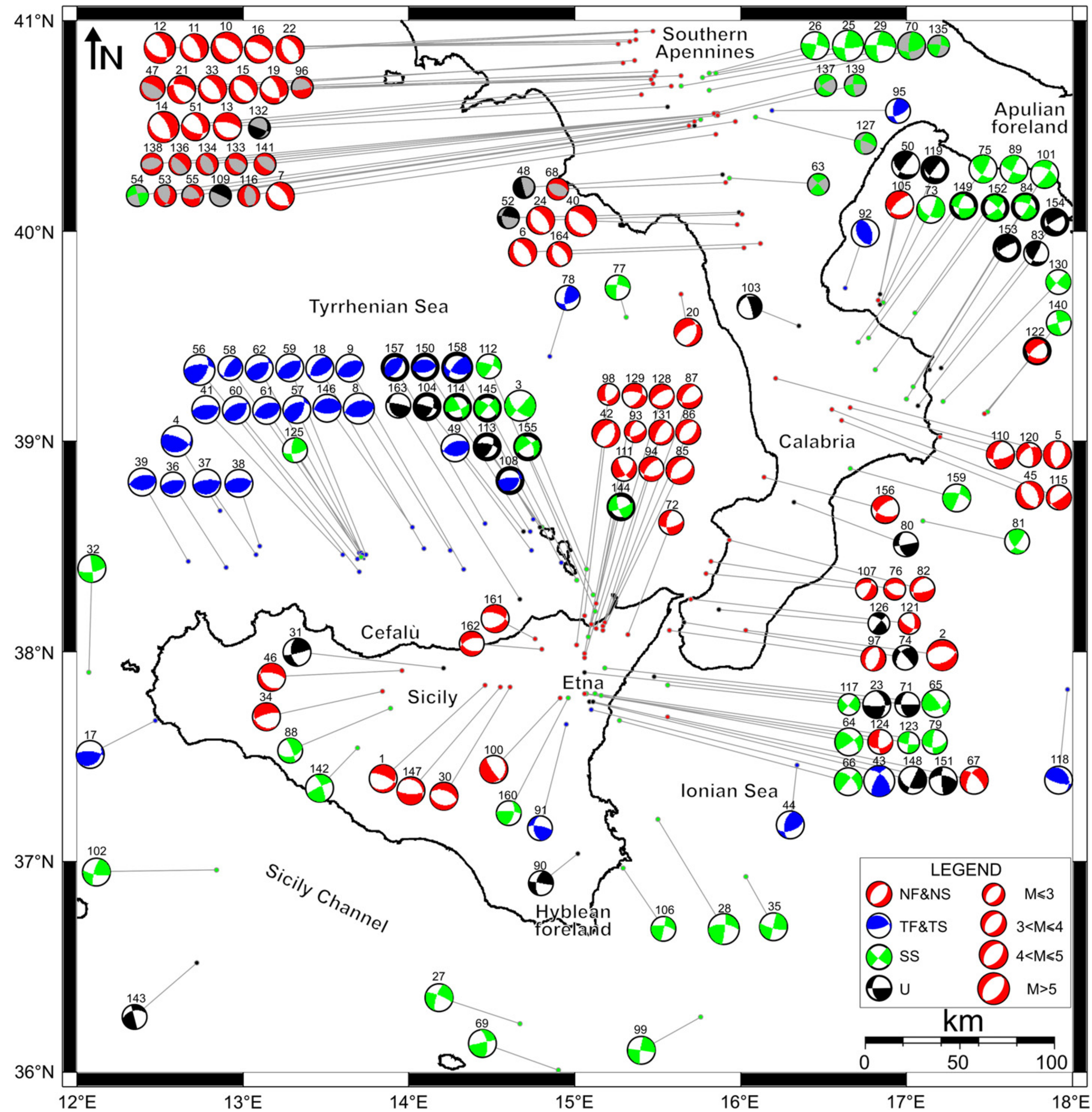

Fig. 4. Selected crustal earthquake focal mechanisms for the large Calabrian Arc area including the southern Apennines, Calabria, Sicily, south-Tyrrhenian, and Sicily Channel (Table 1). Following the classification adopted in the World Stress Map (Zoback, 1992; http://dc-app3-14.gfz-potsdam.de/), different colors identify different types of mechanisms: red = normal faulting (NF) or normal faulting with a minor strike-slip component (NS); green = strike-slip faulting (SS); blue = thrust faulting (TF) or thrust faulting with a minor strike-slip component (TS); black = unknown stress regime (U). White background of beach balls is for mechanisms from waveform analysis, whereas gray background is for mechanisms from P-wave first motions. Thick perimeters of the beach balls are for the 17 new focal mechanisms computed in this work by using the CAP technique. The beach ball size is proportional to the earthquake magnitude (see right side of the legend).

zone linking the central Aeolian Islands to Mt Etna (AIME for brevity). The indentation of the CCMS extensional domain within the AIME strike-slip domain is further addressed, from a tectonic point of view, below in the Discussion section. Toward the northeast, on the other side of the Calabrian extensional domain, strike-slip mechanisms characterize the Ionian coast of central Calabria, where, however, a NW–SE extensional component is also present (Plot 7 in Fig. 5).

In the Southern Apennines, focal mechanisms (Fig. 4) are predominantly normal with nodal planes striking NW–SE and T-axes (Plot 8 in Fig. 5) trending perpendicularly along the regional direction of extension (Montone et al., 2004; Pondrelli et al., 2006). Plot 8 (Fig. 5) shows also the presence of sub-horizontal P-axes trending NW–SE. Most of these events are those pertaining to the Potenza 1990–1991 seismic sequence (Boncio et al., 2007), which was a strike-slip

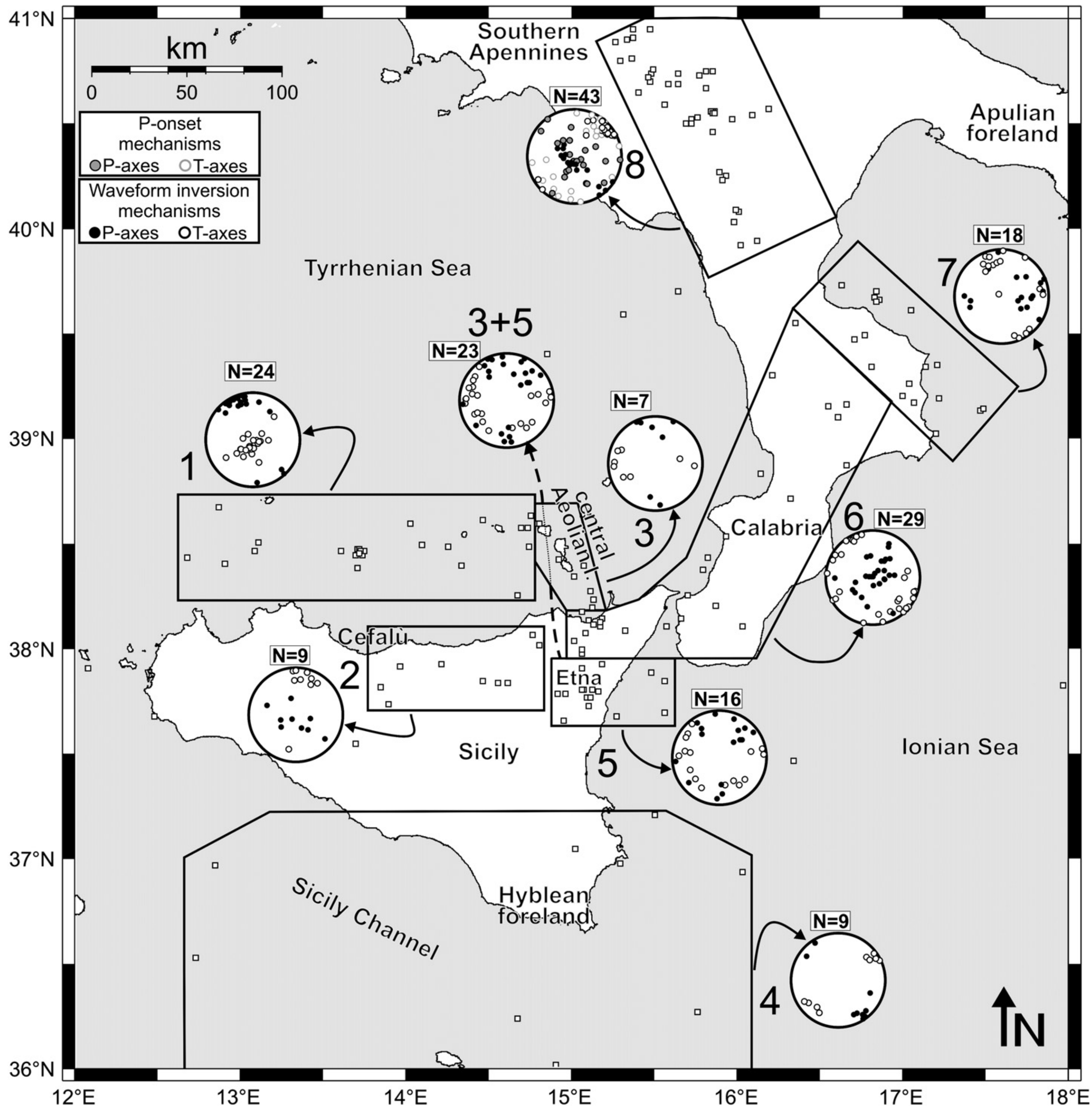

Fig. 5. Polar plots of P- and T-axes for earthquakes grouped by different seismological domains (indicated with black boxes). See the legend for explanation of color codes.

sequence within the active extensional (NE–SW extension) Southern Apennines (see also Frepoli et al., 2011).

The depth distribution of focal mechanisms is shown in Fig. 6 for the main seismogenic zones identified in Fig. 5 and indicated with red lines to be considered as cross-section tracks (see caption to Fig. 6 for details). The available focal depths are mainly between 0 and −20 km. The focal depth distribution seems to well reflect the main features of the lithospheric structure. Earthquakes are mainly clustered at shallow depths (<20 km) beneath the southern Calabria and south-Tyrrhenian areas, where the seismic wave velocity pattern indicates a crustal thinning (e.g., Orecchio et al., 2011 and references therein), whereas earthquakes reach greater depths in the remaining sectors, including the two sectors probably acting as transition zones between different domains (i.e., east-Sicily and north-Calabria; cross-sections 2 and 4 in Fig. 6).

4. Seismogenic stress inversion for the Calabrian arc region

Recent regional-scale investigations of the stress field in southern Italy (Barba et al., 2010; Frepoli and Amato, 2000b; Montone et al., 2004; Pierdominici and Heidbach, 2012) have been performed with the primary support of P-onset polarity focal mechanisms, borehole measurements and fault kinematic indicators, sometimes integrated by a minor contribution of waveform inversion focal mechanisms. Other studies based on use of the same kind of data have mostly focused on small or limited sectors of the Calabrian Arc and adjacent

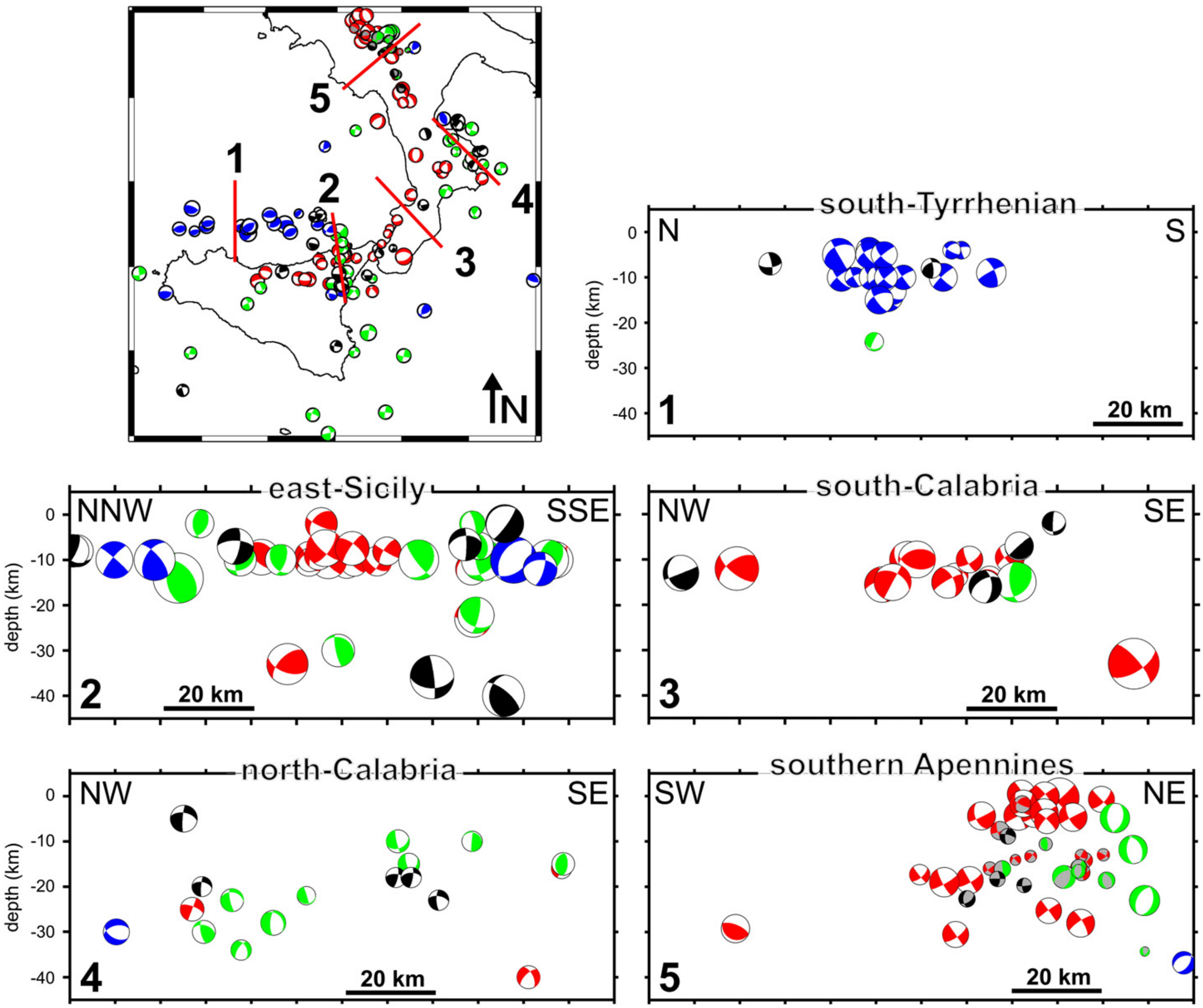

Fig. 6. Depth of focal mechanisms projected along five cross-sections perpendicular to the Calabrian Arc (see cross-section tracks in red). Maximum projection distance is 110, 40, 85, 25, and 85 km for tracks 1, 2, 3, 4, and 5, respectively. White background of beach balls is for mechanisms from waveform analysis, whereas gray background is for mechanisms from P-wave first motions. Red = normal faulting or normal faulting with a minor strike-slip component; green = strike-slip faulting; blue = thrust faulting or thrust faulting with a minor strike-slip component; black = unknown stress regime. The beach ball size is proportional to the earthquake magnitude.

regions (e.g., Alparone et al., 2011; Barberi et al., 2000; Billi et al., 2010b; Boncio et al., 2007; Brozzetti et al., 2009; Frepoli et al., 2011; Giampiccolo et al., 2008; Maggi et al., 2009; Musumeci et al., 2005; Neri et al., 2004; 2005; Pasquale et al., 2009; Sgroi et al., 2012). The main difference between the present study and the previous ones is concerned with the kind and quality of data used. While most focal mechanisms used by the previous investigators were coming from inversion of P-onset polarities, a technique well known to undergo frequent failure and large approximations in regions of poor network geometry like the Calabrian Arc one, we have compiled and used in the present study a more robust database almost exclusively including focal solutions coming from application of the most effective waveform inversion techniques. 60% of the focal mechanisms included in our database have never been used in the previous regional-scale investigations, e.g. our database is substantially new for our application. With the present study we aim (i) to furnish an overall view of the seismotectonics of the entire Calabrian Arc region and (ii) to better explore so far poorly-investigated sectors like, for example, northern Calabria.

We inverted, for stress tensor parameters, sub-samples of focal mechanisms mainly computed through waveform analyses and reported in our database (Table 1, Fig. 7). We applied the method of Gephart and Forsyth (1984) and Gephart (1990), the basic assumptions of which are as follows: (1) stress is uniform in the rock volume investigated, (2) earthquakes are shear dislocations on preexisting faults, and (3) slip occurs in the direction of the resolved shear stress on the fault plane. The algorithm searches for the stress tensor showing the best agreement with the available focal mechanisms. Four stress parameters are calculated, three of them define the orientations of the main stress axes σ1, σ2, and σ3 (maximum, intermediate, and minimum compressive stresses, respectively), the fourth one (R) is a measure of the relative stress magnitudes: $R = (\sigma2 - \sigma1) / (\sigma3 - \sigma1)$. The R parameter ranges from 0 to 1, where low and high R-values indicate a magnitude of the intermediate compressional stress (σ2) close to the maximum (σ1) and minimum (σ3) stresses, respectively. The average misfit (F) between the estimated stress tensor and the fault-plane solutions gives preliminary information about stress homogeneity in the inversion dataset or, equivalently, in the concerned rock volume. Following Wyss et al. (1992) and Gillard et al. (1996), we assumed that the condition of homogeneous stress distribution is fulfilled if the average misfit F is smaller than 6° and that it is not fulfilled if F is greater than 9°. In the 6° < F < 9° range, the solution is considered as acceptable, although it may reflect some heterogeneities. In this latter case, in order to identify sub-volumes as homogeneous as possible, we also run a joint evaluation of the F-value and the individual earthquake misfits. Through a trial and error procedure (e.g. Caccamo et al., 1996; Wyss et al., 1992), when high individual misfits are found for peripheral earthquakes in the inversion volume, the sub-volume boundary is moved to exclude these marginal events and a new inversion is carried out to check the stress uniformity in the new sub-volume. The primary criteria to define the separate inversion volumes (Fig. 7) are the earthquake mechanism similarity and spatial aggregation (see Figs. 4 and 5). The tectonic domains reported in the literature do not necessarily coincide with the space partitioning based on the above criteria, but, in the case of the present study, a general correspondence can be noted between our space partitioning of faulting regimes (Figs. 4, 5 and 7) and the seismotectonic zoning available from previous investigations (Section 2.1).

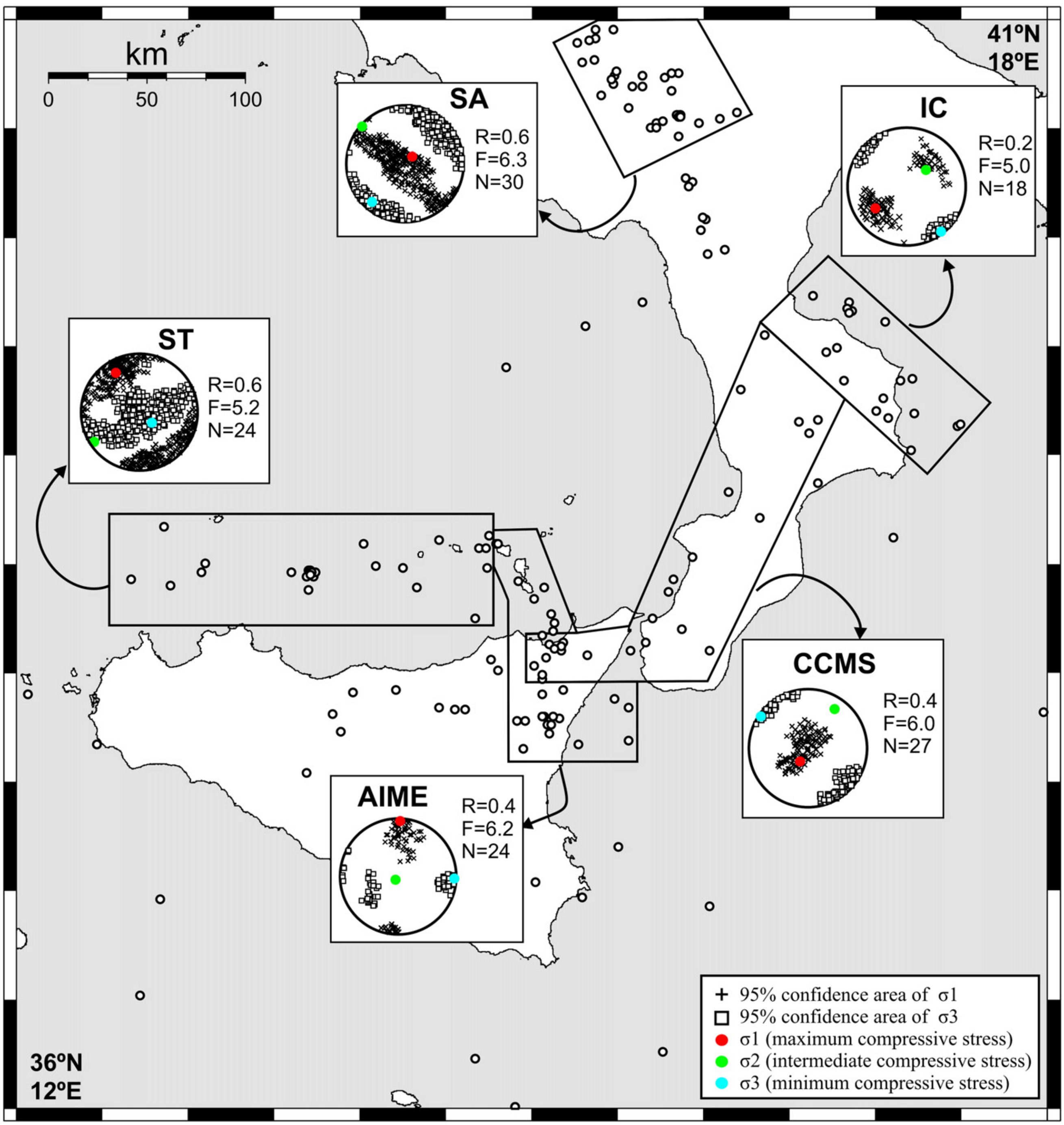

Fig. 7. Orientations of the principal stress axes and other parameters obtained by inversion of the earthquake focal mechanisms in the separate sub-volumes (see also Table 2). Red, green, and blue dots indicate the orientations of the maximum (σ1), intermediate (σ2), and minimum (σ3) compressive stresses, respectively. Crosses and squares indicate the 95% confidence areas for the σ1 and σ3 axes. The 95% confidence area for the σ2 axis is not displayed.

Our results are reported in Fig. 7 and Table 2. Fig. 7 displays the orientations of the main stress axes and the 95% confidence limits of σ1 and σ3 for the five sub-volumes that have furnished a reliable stress field solution, namely, Southern Apennines (SA), Ionian Calabria (IC), Central Calabria to Messina Straits (CCMS), central Aeolian Islands to Mount Etna (AIME), and south-Tyrrhenian (ST). The confidence limits of the solution were computed by using the statistical procedure described by Parker and McNutt (1980) and Gephart and Forsyth (1984).

The F-value of 6.0° and the relatively small 95% confidence limits of the solution found in the sub-volume CCMS (including 27 earthquakes) indicate good levels of stress homogeneity and solution constraint. The steep attitude of σ1 together with a sub-horizontal σ3 trending N304°E defines an extensional stress regime for this domain closely matching geologic and structural evidence (Tortorici et al., 1995a). The prolongation of this extensional domain toward the northeastern corner of Sicily was already fairly evident from the focal mechanisms and the P- and T-axes distribution (Figs. 4 and 5) and is now further confirmed by stress homogeneity in CCMS (Fig. 7).

In the IC sub-volume (Fig. 7), a smaller number of data (18) has not prevented us from finding again a reliable stress tensor solution characterized by a rather small misfit value (F = 5.0°) and rather well constrained 95% confidence areas. The resulting stress field is compatible with a transtensive tectonic regime.

At the northern limb of the Calabrian Arc (sector 8 of Fig. 5), an F-value of 7.1° and rather large confidence areas for the steep σ1 and shallow σ3 axes reveal a dominant extension with a relevant degree of stress heterogeneity in the data set. Following the above described trial and error procedure, more homogeneous sub-volumes have been found separating the northern and southern sectors, similar to what was previously done by more local studies (Frepoli et al., 2011; Maggi et al., 2009). The extensional stress field estimated for the 30 earthquakes of the northernmost sub-volume (SA in Fig. 7) shows a lower misfit value of 6.3° (modest degree of stress heterogeneity), a steep σ1 axis, and a horizontal σ3 axis trending northeast. Stress inversion of the remaining 8 earthquakes located immediately to the south of sector SA (Fig. 7) seems to suggest again an extensional domain but with a slightly rotated direction of extension (σ3 trending ca. NNE–SSW). This latter result needs to be verified with more data in future investigations and is not shown in Fig. 7 for its preliminarity.

In the ST sub-volume (Fig. 7), an F-value of 5.2° is found to be associated with relatively large confidence areas of σ1 and σ3 axes. The sub-horizontal, NW-oriented maximum compressive stress likely reflects the NW–SE Nubia–Eurasia convergence in this sector, in agreement with crustal motion models by Sella et al. (2002), Calais et al. (2003), and Nocquet and Calais (2004). The apparently contrasting low misfit and large confidence limits of the obtained solution can be ascribed to the presence of many nearly identical focal mechanisms in an even acceptably dense dataset, a condition known to bring the inversion matrix close to singular (e.g., Townend and Zoback, 2006; Wyss et al., 1992).

Finally, an F-value of 6.2° (indicating modest degree of stress heterogeneity) and an acceptable 95% confidence areas are obtained for the sector AIME (Fig. 7) coincident with the transcurrent faulting domain “3 + 5” of Fig. 5 (see previous section). In this sub-volume, the horizontal N-trending σ1 suggests a slight rotation of the maximum compressive stress with respect to the adjacent south-Tyrrhenian sub-volume (ST). This rotation can be probably ascribed to the interaction between convergence, dominating on the western side, and rollback-induced extension, dominating on the eastern side (see next section).

In our stress analysis, R values range between 0.6 and 0.4 for four investigated sub-volumes (SA, ST, CCMS and AIME in Fig. 7 and Table 2) indicating that σ2 amplitude is nearly intermediate between σ1 and σ3 amplitudes (true triaxial compression) in these sectors. In the case of sub-volume IC, the R value of 0.2 indicates greater closeness of the σ2 amplitude to the one of σ1, suggesting biaxial deviatoric compression or confined extension (Mandle, 1988).

5. Discussion

In the Calabrian Arc, the earthquake focal mechanisms (Fig. 4), the related P- and T-axes (Fig. 5), and the derived seismogenic stress fields (Fig. 7) define three main seismotectonic domains (Southern Apennines, south-Tyrrhenian, and Central Calabria to Messina Straits; Fig. 8), which are also characterized by rather homogeneous surface or shallow faulting regimes (Fig. 1a). The tectonic relevance of our seismological data is here evaluated also through the comparison with recent GPS data, which are totally independent from our database. The most recent GPS data for the Calabrian Arc are from Serpelloni et al. (2007, 2010), D'Agostino et al. (2008, 2011), Devoti et al. (2008), Billi et al. (2011), and Palano et al. (2011, 2012). Horizontal components of strain-rate fields obtained from least-squares interpolation of the horizontal GPS velocities (Billi et al., 2011) are plotted in Fig. 8 together with the horizontal components of P-, T-, and stress-axes from this paper (Figs. 5 and 7). In particular, Fig. 8 shows the available seismic and GPS axes for the three main seismotectonic domains of the Calabrian Arc region (Southern Apennines, south-Tyrrhenian, and Central Calabria to Messina Straits), where both the seismic and GPS signals are straightforward and where the regional tectonic signal prevails on local ones. A comparison of seismic and geodetic axes shows a good consistency (i.e., parallelism of axes, Fig. 8). Two of these three main domains occupy the wings of the arc (i.e., the Southern Apennines, to the northeast, and the south-Tyrrhenian, to the southwest), whereas the third one (i.e., Central Calabria to Messina Straits) occupies the central portion of the arc. The dimension of these domains (c. 100–250 km in length) suggests that they are connected with regional tectonic mechanisms rather than local ones. Moreover, lithosphere–mantle tomographic images (Fig. 2) show that the central domain corresponds to the area overlying the Ionian slab (i.e., Calabria), whereas the two lateral wings (i.e., Southern Apennines and southern Tyrrhenian) correspond to regions where subduction is now inactive (Di Stefano et al., 2009; Faccenna et al., 2004). The Southern Apennines, in particular, is presently undergoing post-orogenic extension (Figs. 1a, 4, 5, and 7) related to post-orogenic collapse tectonics. The extensional tectonics of Calabria (Figs. 4, 5, and 7) is, in contrast, generally ascribed to the slow slab rollback (D'Agostino et al., 2011). Open questions about this interpretation are discussed below. The compressional tectonics active in the south-Tyrrhenian (Figs. 4, 5, and 7) is ascribed to the general Nubia-Europe convergence in the central Mediterranean and, locally, with a

Table 2
Stress inversion results for earthquake sets analyzed in the present study.

Sub-volume	N	F (°)	R	σ1 Pl (°)	σ1 Az (°)	σ2 Pl (°)	σ2 Az (°)	σ3 Pl (°)	σ3 Az (°)
CCMS	27	6.0	0.4	68	211	26	34	1	304
IC	18	5.0	0.2	35	235	55	49	3	143
AIME	24	6.2	0.4	5	2	84	223	4	92
ST	24	5.2	0.6	22	329	7	237	67	130
SA	30	6.3	0.6	76	45	1	311	14	221

Stress inversion of earthquake focal mechanisms for the sub-volumes shown in Fig. 7. N is the number of inverted earthquakes. F is the average misfit for the best stress model, and $R = (\sigma2 - \sigma1)/(\sigma3 - \sigma1)$ where σ1, σ2, and σ3 represent the amplitudes of the maximum, intermediate and minimum compressive stress, respectively. Pl and Az are plunge and azimuth, respectively, of the three main stress axes.

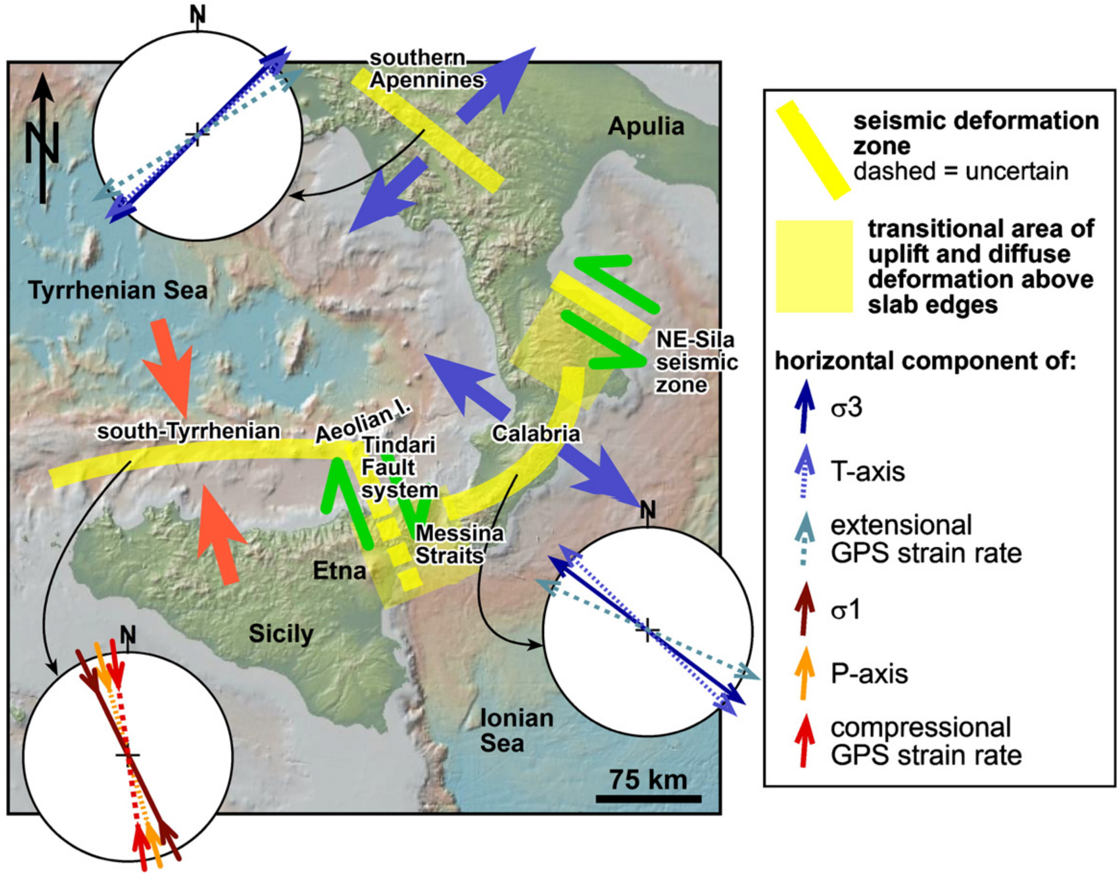

Fig. 8. Seismotectonic synthesis of the Calabrian Arc region. Two transverse seismic zones (Tindari Fault system and NE-Sila zone with associated areas of uplift and diffuse deformation above slab edges) separate three main seismotectonically-heterogeneous deformation zones (Southern Apennines, Calabria and Messina Straits, and south-Tyrrhenian). The southern segment of the Tindari Fault system is dashed because it is uncertain (see text for further explanations). In the polar plots, orientations of P- and T- axes and σ1 and σ3 are from this paper, whereas the horizontal strain-rate fields obtained from least-squares interpolation of the horizontal GPS velocities are from Billi et al. (2011). Note that the seismological and geodetic axes shown in the three polar plots are, in each domain, almost parallel (Southern Apennines, Central Calabria to Messina Straits, and south-Tyrrhenian), thus reciprocally supporting the adopted seismological and geodetic methods and results.

compressional rejuvenation of the Sicilian Apennines (Maghrebides) at the rear of the orogen, due to the locking of the frontal thrust (in southern Sicily and Sicily Channel) connected with the arrival of the African continent in the subduction zone (Billi et al., 2007, 2011; Pepe et al., 2005). It is also true, however, that some compressional (seismic) activity is detected along buried thrusts in the central and frontal part of the Sicilian Maghrebides (Lavecchia et al., 2007a, 2007b). Other seismotectonic domains of the study area, such as the Cefalù–Etna belt, Sicily mainland, and Sicily Channel are not considered here among the main seismotectonic domains (Fig. 8) for the limited number of significant earthquakes that occurred during our recording interval. This evidence, however, does not exclude that also these domains may have been affected in the past or will be affected in the future by significant earthquakes (e.g., Billi et al., 2010b; Chironi et al., 2000; Lavecchia et al., 2007a, 2007b).

The presence, in the Calabrian Arc region, of three main seismotectonic domains, namely Southern Apennines, south-Tyrrhenian, and Central Calabria to Messina Straits (Fig. 8), implies the presence of transfer domains or accommodation zones in the transitional areas between these domains (Fig. 8). One of these transfer domains corresponds to the strike-slip to transtensional Tindari Fault system in northeastern Sicily (Fig. 1a; Billi et al., 2006). Both the P-axes (plot "3 + 5" in Fig. 5) and the computed σ1 (sector AIME in Fig. 7) for this transfer domain trend circa NNE–SSW, which is a rather anomalous trend within the general NW–SE Nubia–Eurasia convergence (e.g., Serpelloni et al., 2007). As above mentioned, this apparently anomalous trend can be explained with a local accommodation tectonics caused by the interaction between convergence, dominating on the western side, and rollback-induced extension, dominating on the eastern side (Negredo et al., 1999; Neri et al., 2005).

The second accommodation zone should be located in the Ionian side of central-northern Calabria, between the different but both extensional seismotectonic domains of Southern Apennines and central Calabria (see NE-Sila seismic zone in Fig. 8). In this sector, strike-slip faults and, more in general, transcurrent tectonics have been documented (e.g., Amodio Morelli et al., 1976; Catalano et al., 1993; Cinque et al., 1993; Del Ben et al., 2008; Ferranti et al., 2009; Galli and Scionti, 2006; Knott and Turco, 1991; Seeber et al., 2008; Speranza et al., 2011; Spina et al., 2009; Van Dijk, 1994), but a well defined and continuous fault zone has not been identified so far; rather, this strike-slip faulting domain seems to consist of a diffuse set of NW- and WNW-striking strike-slip faults, which are at least in part seismically active and are here collectively named as the NE-Sila seismic zone (Fig. 8). Our new focal mechanisms provide new and better constraints on the kinematics of this zone (see Fig. 4 and Table 1) and the first estimate of the local seismogenic stress field (Fig. 7). These new data, in particular, confirm the dominant strike-slip tectonics of the NE-Sila seismic zone and show that the seismogenic stress is oddly oriented (i.e., NW–SE-trending σ3, Fig. 7) with respect to the regional NW–SE Nubia–Eurasia convergence, thus pointing toward a local accommodation tectonics as the main tectonic agent, rather than the regional Nubia–Eurasia convergence. It is also interesting to mention that, despite the fact that faults in the NE-Sila seismic zone are still poorly defined, historical and paleoseismological data from this zone and adjacent ones support the occurrence, during historical times, of magnitude class 6 and class 7 earthquakes possibly along the NW-striking strike-slip faults mentioned above (Galli and Bosi, 2002; Galli and Scionti, 2006).

A comparison between the surface seismotectonic domains of the Calabrian Arc region (Fig. 8) and the lithosphere-mantle tomographic images (Fig. 2) shows that the two above-mentioned transfer domains are located on top of the lateral edges of the retreating Ionian slab (Faccenna et al., 2011). The transfer domains may, therefore, represent the surface expression of a deep tectonics involving the rollback of the Ionian narrow slab toward the southeast. This mechanism would drive the southeastward drift of the overlying Calabrian wedge (only the portion on top of the retreating slab), while the lateral sectors overlying the broken-off slab would not be drifted toward the trench (southeastward), thus provoking a differential kinematics between adjacent compartments of the Calabrian Arc region. This model is supported by recent GPS data showing the differential kinematics along the Calabrian Arc, where only the central part of the arc is currently drifting toward the Ionian Sea (D'Agostino et al., 2011). Govers and Wortel (2005) documented that tear faults and fault zones similar to those above discussed and located near the horizontal terminations of subduction trenches are worldwide rather diffuse (i.e., STEP, Subduction-Transform Edge Propagator faults). In the case studied in this paper, the Tindari Fault system and the NE-Sila seismic zone may represent an expression in the overriding plate of STEP faults underneath located in the subducting plate.

To complete the discussed seismotectonic picture, main unsolved questions concerning the present tectonics of the Calabrian Arc are synthesized as follows.

(1) The first question concerning the Calabrian Arc is about the transfer zones located at the edges of the Ionian slab (i.e., Tindari Fault system and NE-Sila seismic zone) and about the reason why these transfer zones are so different. While the Tindari Fault system is geologically and geophysically rather well defined (in its northern section, at least) and it includes or it is bounded by large volcanic provinces such as Mt Etna and the Aeolian volcanoes (see following points for open questions about this transfer zone), the NE-Sila seismic zone includes some WNW-striking active faults, which are still poorly defined and whose surface geological expression is still weak. One explanation may be that this latter transfer zone is poorly developed due, for instance, to small deformations (and therefore small average deformation rates) along it. Speranza et al. (2011) suggest that the onset of this fault zone occurred around 1.2 Ma or in younger times, which is comparable with the hypothesized onset age of the Tindari Fault system (0.5–1.0 Ma; Billi et al., 2006). This explanation is consistent with recent GPS data. As shown by D'Agostino et al. (2011), the differential kinematics of adjacent domains inducing strike-slip accommodation along the Tindari Fault system is larger (in terms of slip rate deduced from GPS velocities) than the one along the NE-Sila seismic zone. In other words, different deformation rates may be the cause or one of the causes of the tectonic differences on top of the southwestern and northeastern edges of the Ionian slab (i.e., Tindari Fault system and NE-Sila seismic zone). This differential tectonics remains, however, to be largely understood and further explored, but our new focal mechanisms, at least, contribute to better understand the kinematics and dynamics of the NE-Sila seismic zone.
(2) The Tindari Fault system is rather well defined by geological and geophysical evidence only in its offshore and coastal (i.e., northern) sections, whereas toward the south (i.e., toward Mt Etna) the evidence of a single discrete fault system fades away (Billi et al., 2006). Nonetheless, this area is very active and hosts several earthquakes in addition to the volcanically-active area of Mt Etna, below which strike-slip earthquakes are also frequent (Figs. 1b and 4). In particular, in Figs. 5 and 7, we have shown that the seismic belt running NNW–SSE from the central Aeolian Islands to Mt Etna (through Tindari) is seismologically heterogeneous including right-lateral strike-slip and extensional-to-transtensional events, these latter earthquakes being compatible with the seismological domain of Central Calabria to Messina Straits (Figs. 5 and 7). To overcome the heterogeneous deformation pattern of northeastern Sicily, Goes et al. (2004) proposed that, toward the south, the Tindari Fault changes from a concentrated to a diffuse lateral margin of the Calabrian domain, including in this diffuse margin also the Messina Straits. This hypothesis is a viable one, but still rather speculative. Recently, Billi et al. (2010b) and Faccenna et al. (2011) emphasized the role of rapid uplift in the Messina Straits area and abundant magmatism below Mt Etna in this tectonically complex corner of the Calabrian Arc, but the exact role of both these mechanisms on the surface tectonics remains to be further constrained. Additional details about the role of uplift are given in the following point. On their hand, GPS data show a sharp kinematic jump across the Messina Straits (D'Agostino and Selvaggi, 2004; Serpelloni et al., 2010), suggesting that this area may be a part of the accommodation zone between the Calabrian and south-Tyrrhenian domains, as also proposed by Goes et al. (2004).
(3) Calabria and northeastern Sicily are rapidly uplifting areas, which have undergone significant uplift during Quaternary time (Antonioli et al., 2006; Lambeck et al., 2004; Molin et al., 2004; Olivetti et al., 2012). Faccenna et al. (2011) emphasized that vertical motions are particularly remarkable above the edges of the Ionian slab (i.e., in the Sila Massif and in northeastern Sicily) and ascribed this observation to the effect of mantle return flows ascending around the Ionian slab edges. Constraining these mantle flows and their surface effects is obviously very complicated, but these flows may explain at least in part the diffuse, poorly defined system of faults occurring over both edges of the Ionian slab (i.e., along the southern prolongation of the Tindari Fault and along the NE-Sila seismic zone). According to this model, deformations occurring above the edges of the Ionian slab are not simply synthesizable in narrow fault zones accommodating horizontal slip. Vertical motions possibly connected with complex mantle flows around slab edges may significantly complicate the kinematic framework above slab edges and induce deformations in significantly large regions (Fig. 8). In the case of the Calabrian Arc, the surface areas involved in the mechanisms occurring at the slab edges may be a large part of the Sila Massif and surrounding areas, to the northeast, and the Messina Straits and a large part of northeastern Sicily including Mt Etna, to the southwest (Faccenna et al., 2011). As explained by Billi et al. (2010b) and Faccenna et al. (2011), flows below Mt Etna may explain mantle upwelling and volcanism and also thermo-mechanical lithospheric erosion and thinning close to Mt Etna (Miller and Piana Agostinetti, 2011). Mantle upwelling, in turn, could be responsible for the radial pattern of some important active extensional faults around Mt Etna (Fig. 1), including the Cefalù–Etna seismic zone, the northern portion of the Malta escarpment (and associated parallel faults), the Messina Straits faults, and the faults along the southern prolongation of the Tindari Fault (Billi et al., 2010b).
(4) In contrast with the extensional Southern Apennines and compressional south-Tyrrhenian domains, where the seismotectonic activity is characterized by frequent earthquakes, in the extensional domain of Calabria (i.e., above the subducting Ionian slab) less frequent events have so far occurred. This seismic behavior may be explained with a substantial post-seismic phase following the strong earthquakes and earthquake sequences of 1783, 1894, 1905, 1907, and 1908 (Neri et al., 2006). It is also true, however, that the retreat of the nearly vertical Ionian slab (Fig. 2) is very slow, almost ceased (D'Agostino et al., 2011). Within this tectonic framework, the extensional deformation (and

rate) of Calabria connected with the slab retreat should be minimal. Therefore, to explain the above-mentioned strong historical earthquakes of Calabria, we have to invoke very long return times of earthquakes (i.e., because of an assumed slow deformation rate induced by the slow slab rollback), or, alternatively, we have to invoke an additional tectonic mechanism inducing extension in Calabria, such as its rapid uplift or differential uplifts in adjacent sectors of Calabria (Faccenna et al., 2011). This may explain also particular structures in Calabria such as the Lamezia–Catanzaro transverse valley bordered by WNW–ESE-striking normal faults (see also Reitz and Seeber, 2012, for a model of arc-parallel strain).

(5) The occurrence of strike-slip earthquakes in the extensional seismic belt of Southern Apennines (Fig. 4) is surely one of the open tectonic questions of the Calabrian Arc and it is addressed in Boncio et al. (2007), who invoke inherited E–W-striking crustal (or possibly lithospheric) fault zones that can be reactivated in strike-slip motion under the present stress field of the Southern Apennines.

(6) Deep crustal earthquakes (between about 25 and 40 km; Fig. 6) are more frequent in the Southern Apennines and along the Tindari and NE-Sila seismic zones (Fig. 6). Probably, the simplest explanation for this observation may be that these earthquakes occur in the Southern Apennines, for the marked crustal doubling of this region (Scrocca et al., 2005), and along the Tindari and NE-Sila seismic zones, for the effect of STEP faults active below, in the subducting plate. On the other hand, the stretched and warm crust of south-Tyrrhenian will difficultly host deep crustal earthquakes, which are also absent in the Tyrrhenian side of Calabria (Fig. 6).

6. Conclusions

Selection and stress inversion of the best quality shallow earthquake focal mechanisms available from catalogs and the literature (147 solutions) and from this work (17), 60% of which never used before for regional-scale geodynamic investigations, have allowed us to improve the knowledge of the main seismotectonic domains in the Calabrian Arc region, evidencing at the same time some critical situations which are still poorly understood and should be better investigated in the future. An extensional domain with minimum compressive stress ($\sigma3$) oriented WNW–ESE is detected in the central section of the Arc (Central Calabria to Messina Straits) on top of the southeastward-retreating Ionian subducting slab. To the southwest (Southern Tyrrhenian domain) and to the north (Southern Apennines) of this extensional domain, where slab break-off occurred and active subduction is therefore substantially absent, different seismogenic stress tensors are estimated: (1) a compressional stress regime compatible with the NW–SE plate convergence is found in the Southern Tyrrhenian domain and (2) an extensional stress regime compatible with the post-orogenic NE–SW extension affecting the entire Apenninic chain is detected in the Southern Apennines. Dynamic regimes compatible with transcurrent kinematics, dextral and sinistral, respectively, have been found to be dominant in the Tindari and the NE-Sila seismogenic zones. These transitional transcurrent zones are located on top of the Ionian slab edges, appear to be forced in their horizontal transfer kinematics by the different tectonic regimes occurring in the adjacent compartments, and are here considered as possible expressions in the overriding plate of Subduction-Tranform Edge Propagator (STEP) faults occurring underneath in the subducting plate. A set of open questions concerning the present tectonics of the Calabrian Arc reported in this paper may serve as a guide for future studies.

Acknowledgments

This work was realized within the framework of the TopoMed Project led by R. Wortel. TopoMed is part of the ESF EUROCORES Topo-Europe Programme (www.topo-europe.eu) led by S. Cloetingh. Some Figures were created using the Generic Mapping Tools (GMT) by Wessel and Smith (1991). We warmly thank the Editor, his staff, and anonymous reviewers for a very constructive work on our manuscript.

References

Aloisi, M., Cocina, O., Neri, G., Orecchio, B., Privitera, E., 2002. Seismic tomography of the crust underneath the Etna volcano, Sicily. Physics of the Earth and Planetary Interiors 134, 139–155.

Alparone, S., Barberi, G., Bonforte, A., Maiolino, V., Ursino, A., 2011. Evidence of multiple strani fields beneath the eastern flank of Mt. Etna volcano (Sicily, Italy) deduced from seismic and geodetic data during 2003–2004. Bulletin of Volcanology 73, 869–885.

Alvarez, W., Cocozza, T., Wezel, F.C., 1974. Fragmentation of the Alpine orogenic belt by microplate dispersal. Nature 248, 309–314.

Amicucci, L., Barchi, M.R., Montone, P., Rubiliani, N., 2008. The Vallo di Diano and Auletta extensional basins in the southern Apennines (Italy): a simple model for a complex setting. Terra Nova 20, 475–482. http://dx.doi.org/10.1111/j.1365- 3121.2008.00841.x.

Amodio Morelli, L., Bonardi, G., Colonna, V., Dietrich, D., Giunta, G., Ippolito, F., Liguori, V., Lorenzoni, S., Paglionico, A., Perrone, A., Piccaretta, G., Russo, M., Scandone, P., Zanettin-Lorenzoni, E., Zuppetta, A., 1976. L'arco Calabro-Peloritano nell'orogene Appenninico-Maghrebide. Memorie della Società Geologica Italiana 17, 1–60.

Amoruso, A., Crescentini, L., Scarpa, R., 2002. Source parameters of the 1908 Messina Straits, Italy, earthquake from geodetic and seismic data. Journal of Geophysical Research 107, B4. http://dx.doi.org/10.1029/2001JB000434.

Amoruso, A., Crescentini, L., Neri, G., Orecchio, B., Scarpa, R., 2006. Spatial relation between the 1908 Messina Straits earthquake slip and recent earthquake distribution. Geophysical Research Letters 33. http://dx.doi.org/10.1029/2006GL027227.

Anderson, H., Jackson, J., 1987. Active tectonics of the Adriatic region. Geophysical Journal of the Royal Astronomical Society 91, 937–983.

Anderson, H., Webb, T., Jackson, J., 1993. Focal mechanisms of large earthquakes in the south-island of New-Zealand — implications for the accommodation of Pacific-Australia plate motion. Geophysical Journal International 115, 1032–1054. http://dx.doi.org/10.1111/j.1365-246X.1993.tb01508.x.

Antonioli, F., Ferranti, L., Lambeck, K., Kershaw, S., Verrubbi, V., Dai, Pra G., 2006. Late Pleistocene to Holocene record of changing uplift rates in southern Calabria and northeastern Sicily (southern Italy, central Mediterranean Sea). Tectonophysics 422, 23–40. http://dx.doi.org/10.1016/j.tecto.2006.05.003.

Arrigo, G., Roumelioti, Z., Benetatos, C., Kiratzi, A., Bottari, A., Neri, G., Termini, D., Gorini, A., Marcucci, S., 2006. A source study of the 9 September 1998 (Mw 5.6) Castelluccio Earthquake in Southern Italy using teleseismic and strong motion data. Natural Hazards 37, 245–262.

Ascione, A., Cinque, A., Improta, L., Villani, F., 2003. Late quaternary faulting within the southern Apennines seismic belt: new data from Mt. Marzano area (Southern Italy). Quaternary International 101–102, 27–41.

Ascione, A., Ciarcia, S., Di Donato, V., Mazzoli, S., Vitale, S., 2012. The Pliocene–Quaternary wedge-top basins of southern Italy: an expression of propagating lateral slab tear beneath the Apennines. Basin Research 24 (4), 456–474. http://dx.doi.org/10.1111/j.1365-2117.2011.00534.x.

Azzaro, R., Barbano, M.S., Camassi, R., D'Amico, S., Mostaccio, A., Piangiamore, G., Scarfì, L., 2004. The earthquake of 6 September 2002 and the seismic history of Palermo (northern Sicily, Italy): implications for the seismic hazard assessment of the city. Journal of Seismology 8, 525–543.

Barba, S., Carafa, M., Mariucci, M.T., Montone, P., Pierdominici, S., 2010. Present-day stress-field modelling of southern Italy constrained by stress and GPS data. Tectonophysics 482, 193–204.

Barberi, F., Civetta, L., Gasparini, P., Innocenti, F., Scandone, R., Villari, L., 1974. Evolution of a section of the Africa-Europe plate boundary: paleomagnetic and vulcanological evidence from Sicily. Earth and Planetary Science Letters 22, 123–132.

Barberi, G., Cocina, O., Neri, G., Privitera, E., Spampinato, S., 2000. Volcanological inferences from seismic-strain tensor computations at Mt. Etna Volcano, Sicily. Bulletin of Volcanology 62, 318–330.

Barberi, G., Cosentino, M.T., Gervasi, A., Guerra, I., Neri, G., Orecchio, B., 2004. Crustal seismic tomography in the Calabrian Arc region, south Italy. Physics of the Earth and Planetary Interiors 147, 297–314.

Barberi, G., Beranzoli, L., Favali, P., Neri, G., Sgroi, T., 2006. Seismic location improvements from an OBS/H temporary network in Southern Tyrrhenian Sea. Annals of Geophysics 49, 2–3.

Barchi, M., Amato, A., Cippitelli, G., Merlini, S., Montone, P., 2007. Extensional tectonics and seismicity in the axial zone of the Southern Apennines. Italian Journal of Geosciences, Special Issue 7, 47–56.

Barreca, G., Barbano, M.S., Carbone, S., Monaco, C., 2010. Archaeological evidence for Romanage faulting in central-northern Sicily: possible effects of coseismic defomation. The Geological Society Special Paper 471, 223–232.

Basili, R., Valensise, G., Vannoli, P., Burrato, P., Fracassi, U., Mariano, S., Tiberti, M.M., Boschi, E., 2008. The Database of Individual Seismogenic Sources (DISS), version 3: summarizing 20 years of research on Italy's earthquake geology. Tectonophysics. http://dx.doi.org/10.1016/j.tecto.2007.04.014.

Bevington, P.R., Robinson, D.K., 2003. Data Reduction and Error Analysis. McGraw-Hill, New York.

Bianca, M., Monaco, C., Tortorici, L., Cernobori, L., 1999. Quaternary normal faulting in southeastern Sicily (Italy): a seismic source for the 1693 large earthquake. Geophysical Journal International 139, 370–394.

Billi, A., Barberi, G., Faccenna, C., Neri, G., Pepe, F., Sulli, A., 2006. Tectonics and seismicity of the Tindari fault system, southern Italy: crustal deformations at the transition between ongoing contractional and extensional domains located above the edge of a subducting slab. Tectonics 25, TC2006. http://dx.doi.org/10.1029/2004TC001763.

Billi, A., Presti, D., Faccenna, C., Neri, G., Orecchio, B., 2007. Seismotectonics of the Nubia plate compressive margin in the south-Tyrrhenian region, Italy: clues for subduction inception. Journal of Geophysical Research 112, B08302. http://dx.doi.org/10.1029/2006JB004837.

Billi, A., Funiciello, R., Minelli, L., Faccenna, C., Neri, G., Orecchio, B., Presti, D., 2008. On the cause of the 1908 Messina tsunami, Southern Italy. Geophysical Research Letters 35, L06301. http://dx.doi.org/10.1029/2008GL033251.

Billi, A., Minelli, L., Orecchio, B., Presti, D., 2009a. Runup distribution for the 1908 Messina tsunami, Italy: observed data versus expected curves. Bulletin of the Seismological Society of America 99, 3502–3509.

Billi, A., Funiciello, R., Minelli, L., Faccenna, C., Neri, G., Orecchio, B., Presti, D., 2009b. Reply to comment by Andrea Argnani et al. on "On the cause of the 1908 Messina tsunami, Southern Italy". Geophysical Research Letters 36, L13308. http://dx.doi.org/10.1029/2009GL037499.

Billi, A., Minelli, L., Orecchio, D., Presti, D., 2010a. Constraints to the cause of three historical tsunamis (1908, 1783, and 1693) in the Messina Straits region, Sicily, southern Italy. Seismological Research Letters 81, 907–915.

Billi, A., Presti, D., Orecchio, B., Faccenna, C., Neri, G., 2010b. Incipient extension along the active convergent margin of Nubia in Sicily, Italy: Cefalù–Etna seismic zone. Tectonics 29, TC4026. http://dx.doi.org/10.1029/2009TC002559.

Billi, A., Faccenna, C., Bellier, O., Minelli, L., Neri, G., Piromallo, C., Presti, D., Scrocca, D., Serpelloni, E., 2011. Recent tectonic reorganization of the Nubia–Eurasia convergent boundary heading for the closure of the western Mediterranean. Bulletin de la Société Géologique de France 182, 279–303.

Bonanno, A., Palano, M., Privitera, E., Gresta, S., Pugliesi, G., 2011. Magma intrusion mechanisms and redistribution of seismogenic stress at Mt. Etna volcano (1997–1998). Terra Nova. http://dx.doi.org/10.1111/j.1365-3121.2011.01019.x.

Bonardi, G., Cavazza, W., Perrone, V., Rossi, S., 2001. Calabria–Peloritani terrane and Northern Ionian Sea. In: Martini, L.P., Vai, G.B. (Eds.), Anatomy of a Mountain Chain: The Apennines and Adjacent Mediterranean Basins. Kluwer, Bodmin, pp. 287–306.

Boncio, P., Mancini, T., Lavecchia, G., Selvaggi, G., 2007. Seismotectonics of strike-slip earthquakes within the deep crust of southern Italy: geometry, kinematics, stress field and crustal rheology of the Potenza 1990–1991 seismic sequence (Mmax 5.7). Tectonophysics 445, 281–300.

Boschi, E., Pantosti, D., Valensise, G., 1989. Modello di sorgente per il terremoto di Messina del 1908 ed evoluzione recente dell'area dello Stretto. Proceedings VIII Meeting Gruppo Nazionale di Geofisica della Terra Solida, Rome, pp. 245–258.

Bottari, A., Capuano, P., De Natale, G., Gasparini, P., Neri, G., Pingue, F., Scarpa, R., 1989. Source parameters of earthquakes in the Strait of Messina, Italy, during this century. Tectonophysics 166, 221–234.

Brozzetti, F., 2011. The Campania–Lucania extensional fault system (southern Italy): a suggestion for a uniform model of active extension in the Italian Apennines. Tectonics 30, TC5009. http://dx.doi.org/10.1029/2010TC002794.

Brozzetti, F., Lavecchia, G., Mancini, G., Milana, G., Cardinali, M., 2009. Analysis of the 9 September 1998 Mw 5.6 Mercure earthquake sequence (Southern Apennines, Italy): a multidisciplinary approach. Tectonophysics 476 (1–2), 210–225.

Butler, R.W.H., Grasso, M., 1993. Tectonic controls on base level variations and depositional sequences within thrust-top and foredeep basins: examples from the Neogene thrust belt of central Sicily. Basin Research 5, 137–151.

Caccamo, D., Neri, G., Saraò, A., Wyss, M., 1996. Estimates of stress directions by inversion of earthquake fault-plane solutions in Sicily. Geophysical Journal International 125, 857–868.

Calais, E., DeMets, C., Nocquet, J.M., 2003. Evidence for a post- 3.16-Ma change in Nubia–Eurasia–North America plate motions? Earth and Planetary Science Letters 216, 81–92.

Carminati, E., Wortel, R., Spakman, W., Sabadini, R., 1998. The role of slab-detachment processes in the opening of the western-central Mediterranean basins: some geological and geophysical evidence. Earth and Planetary Science Letters 160, 651–665.

Carminati, E., Lustrino, M., Cuffaro, M., Doglioni, C., 2010. Tectonics, magmatism and geodynamics of Italy: what we know and what we imagine. Journal of the Virtual Explorer 36. http://dx.doi.org/10.3809/jvirtex.2010.00226.

Carminati, E., Lustrino, M., Doglioni, C., 2012. Geodynamic evolution of the central and western Mediterranean: tectonics vs. igneous petrology constraints. Tectonophysics. http://dx.doi.org/10.1016/j.tecto.2012.01.026.

Catalano, R., D'Argenio, B., 1978. An essay of palinspastic restoration across the western Sicily. Geologica Romana 17, 145–159.

Catalano, S., Monaco, C., Tortorici, L., 1993. Pleistocene strike-slip tectonics in the Lucanian Apennine (Southern Italy). Tectonics 12 (3), 656–665.

Catalano, R., Di Stefano, P., Sulli, A., Vitale, F.P., 1996. Paleogeography and structure of the central Mediterranean: Sicily and its offshore area. Tectonophysics 260, 291–323. http://dx.doi.org/10.1016/0040-1951(95)00196-4.

Catalano, R., Doglioni, C., Merlini, S., 2001. On the Mesozoic Ionian Basin. Geophysical Journal International 144, 49–64.

Catalano, S., De Guidi, G., Monaco, C., Tortrici, G., Tortrici, L., 2008. Active faulting and seismicity along the Siculo-Calabrian Rift Zone (southern Italy). Tectonophysics 453, 177–192.

Cello, G., Guerra, I., Tortorici, L., Turco, E., Scarpa, R., 1982. Geometry of the neotectonic stress field in southern Italy: geological and seismological evidence. Journal of Structural Geology 4, 385–393.

Chevrot, S., Sylvander, M., Delouis, B., 2011. A preliminary catalogue of moment tensors for the Pyrenees. Tectonophysics 510 (1–2), 239–251. http://dx.doi.org/10.1016/j.tecto.2011.07.011.

Chiarabba, C., Jovane, L., Di Stefano, R., 2005. A new view of Italian seismicity using 20 years of instrumental recordings. Tectonophysics 395, 251–268.

Chiarabba, C., De Gori, P., Speranza, F., 2008. The Southern Tyrrhenian subduction zone: deep geometry, magmatism and Plio-Pleistocene evolution. Earth and Planetary Science Letters 268, 408–423. http://dx.doi.org/10.1016/j.epsl.2008.01.036.

Chironi, C., De Luca, L., Guerra, I., Luzio, D., Moretti, A., Vitale, M., Sea Land Group, 2000. Crustal structures of the Southern Tyrrhenian Sea and the Sicily Channel on the basis of the M25, M26, M28, M39 WARR profiles. Bollettino della Societa Geologica Italiana 119, 189–203.

Cifelli, F., Rossetti, F., Mattei, M., 2007. The architecture of brittle postorogenic extension: results from an integrated structural and paleomagnetic study in North Calabria (Southern Italy). Geological Society of America Bulletin 119, 221–239. http://dx.doi.org/10.1130/B25900.1.

Cifelli, F., Mattei, M., Della Seta, M., 2008. Calabrian Arc oroclinal bending: the role of subduction. Tectonics 27 (5), TC5001.

Cinque, A., Patacca, E., Scandone, P., Tozzi, M., 1993. Quaternary kinematic evolution of the southern Apennine. Relationships between surface geological features and deep lithospheric structures. Annali di Geofisica 36, 249–260.

Cinti, F.R., Cucci, L., Pantosti, D., D'Addezio, G., Meghraoui, M., 1997. A major seismogenic fault in a "silent area": the Castrovillari Fault (southern Apennines, Italy). Geophysical Journal International 130, 595–605.

Cinti, F.R., Faenza, L., Marzocchi, W., Montone, P., 2004. Probability map of the next M ≥ 5.5 earthquakes in Italy. Geochemistry, Geophysics, Geosystems 5, Q11003. http://dx.doi.org/10.1029/2004GC000724.

Civello, S., Margheriti, L., 2004. Toroidal mantle flow around the Calabrian slab (Italy) from SKS splitting. Geophysical Research Letters 31, L10601. http://dx.doi.org/10.1029/2004GL019607.

Cloetingh, S.A.P.L., Ziegler, P.A., Bogaard, P.J.F., Andriessen, P.A.M., Artemieva, I.M., Bada, G., Balen, R.T., Beekman, F., Ben-Avraham, Z., Brun, J.P., Bunge, H.P., Burov, E.B., Carbonell, R., Faccenna, C., Friedrich, A., Gallart, J., Green, A.J., Heidbach, O., Jones, A.G., Matenco, L., Mosar, J., Oncken, O., Pascal, C., Peters, G., Sliaupa, S., Soesoo, A., Spakman, W., Stephenson, R.A., Thybo, H., Torsvik, T., de Vicente, G., Wenzel, F., Wortel, M.J.R., 2007. TOPO-EUROPE: the geoscience of coupled deep Earth-surface processes. Global and Planetary Change 85, 1–118.

Cloetingh, S.A.P.L., Thybo, H., Faccenna, C., 2009. TOPO-EUROPE: studying continental topography and deep Earth-surface processes in 4D. Tectonophysics 474, 4–32.

Cloetingh, S.A.P.L., Gallart, J., de Vicente, G., Matenco, L., 2011. TOPO-EUROPE: from Iberia to the Carpathians and analogues. Tectonophysics 502, 1–27.

Cocina, O., Neri, G., Privitera, E., Spampinato, S., 1997. Stress tensor computations in the Mount Etna area (Southern Italy) and tectonic implications. Journal of Geodynamics 23 (2), 109–127.

Cocina, O., Neri, G., Privitera, E., Spampinato, S., 1998. Seismogenic stress field beneath Mt. Etna (South Italy) and possible relationships with volcano-tectonic features. Journal of Volcanology and Geothermal Research 83, 335–348.

Cristofolini, R., Ghisetti, F., Scarpa, R., Mezzani, L., 1985. Character of stress field in the Calabrian Arc and Southern Apennines (Italy) as deduced by geological, seismological and volcanological information. Tectonophysics 117, 39–58.

Cucci, L., 2004. Raised marine terraces in the Northern Calabrian Arc (Southern Italy): a 600 kyr-long geological record of regional uplift. Annals of Geophysics 47, 1391–1406.

Cuffaro, M., Riguzzi, F., Scrocca, D., Dogliosi, C., 2011. Coexisting tectonic settings: the example of the southern Tyrrhenian Sea. International Journal of Earth Sciences 100, 1915–1924.

D'Agostino, N., Selvaggi, G., 2004. Crustal motion along the Eurasia–Nubia plate boundary in the Calabrian Arc and Sicily and active extension in the Messina Straits from GPS measurements. Journal of Geophysical Research 109, B11402. http://dx.doi.org/10.1029/2004JB002998.

D'Agostino, N., Avallone, A., Cheloni, D., D'Anastasio, E., Mantenuto, S., Selvaggi, G., 2008. Active tectonics of the Adriatic region from GPS and earthquake slip vectors. Journal of Geophysical Research 113, B12413. http://dx.doi.org/10.1029/2008JB005860.

D'Agostino, N., D'Anastasio, E., Gervasi, A., Guerra, I., Nedimović, M.R., Seeber, L., Steckler, M., 2011. Forearc extension and slow rollback of the Calabria Arc from GPS measurements. Geophysical Research Letters 38, L17304. http://dx.doi.org/10.1029/2011GL048270.

D'Amico, S., Orecchio, B., Presti, D., Zhu, L., Herrmann, R.B., Neri, G., 2010. Broadband waveform inversion of moderate earthquakes in the Messina Straits, southern Italy. Physics of the Earth and Planetary Interiors 179, 97–106.

D'Amico, S., Orecchio, B., Presti, D., Gervasi, A., Zhu, L., Guerra, I., Neri, G., Herrmann, R.B., 2011. Testing the stability of moment tensor solutions for small earthquakes in the Calabro-Peloritan Arc region (southern Italy). Bollettino di Geofisica Teorica ed Applicata 52 (2), 283–298.

Del Ben, A., Barnaba, C., Toboga, A., 2008. Strike-slip systems as the main tectonic features in the Plio-Quaternary kinematics of the Calabrian Arc. Marine Geophysical Research 29, 1–12. http://dx.doi.org/10.1007/s11001-007-9041-6.

Devoti, R., Riguzzi, F., Cuffaro, M., Doglioni, C., 2008. New GPS constraints on the kinematics of the Apennines subduction. Earth and Planetary Science Letters 273, 163–174.

Devoti, R., Esposito, A., Pietrantonio, G., Pisani, A.R., Riguzzi, F., 2011. Evidence of large scale deformation patterns from GPS data in the Italian subduction boundary. Earth and Planetary Science Letters 311, 230–241.

Dewey, J.F., Helman, M.L., Turco, E., Hutton, D.H.W., Knott, D., 1989. Kinematics of the western Mediterranean. In: Coward, M.P., Dietrich, D., Park, R.G. (Eds.), Alpine Tectonics: Geol. Soc. Spec. Publ., 45, pp. 265–283.

Di Stefano, R., Kissling, E., Chiarabba, C., Amato, A., Giardini, D., 2009. Shallow subduction beneath Italy: three-dimensional images of the Adriatic-European-Tyrrhenian lithosphere system based on high-quality P wave arrival times. Journal of Geophysical Research 114, B05305. http://dx.doi.org/10.1029/2008JB005641.

DISS Working Group, 2007. Database of Individual Seismogenic Sources (DISS) Version 3.0.4: A Compilation of Potential Sources for Earthquakes Larger than M 5. 5 in Italy and Surrounding Areas. ©INGV 2007—Istituto Nazionale di Geofisica e Vulcanologia, Roma (http://www.ingv.it/DISS/).

Doglioni, C., Ligi, M., Scrocca, D., Bigi, S., Bortoluzzi, G., Carminati, E., Cuffaro, M., D'Oriano, F., Forleo, V., Muccini, F., Riguzzi, F., 2012. The tectonic puzzle of the Messina area (Southern Italy): insights from new seismic reflection data. Scientific Reports 2, 970. http://dx.doi.org/10.1038/srep00970.

Dreger, D., 2003. TDMT_INV: Time Domain Seismic Moment Tensor INVersion. International Handbook of Earthquake and Engineering Seismology 81B, 1627.

Dreger, D.S., Helmberger, D.V., 1993. Determination of source parameters at regional distances with 3-component sparse network data. Journal of Geophysical Research — Solid Earth 98 (B5), 8107–8125. http://dx.doi.org/10.1029/93JB00023.

Dvorkin, J., Nur, A., Mavko, G., Ben Avraham, Z., 1993. Narrow subducting slabs and the origin of backarc basins. Tectonophysics 227, 63–79.

Dziewonski, A.M., Chou, T.A., Woodhouse, J.H., 1981. Determination of earthquake source parameters from waveform data for studies of global and regional seismicity. Journal of Geophysical Research 86, 2825–2852.

Ekström, G., England, P., 1989. Seismic strain rates in regions of distributed continental deformation. Journal of Geophysical Research 94, 10231–10257.

Ekström, G., Dziewonski, A.M., Maternovskaya, N.N., Nettles, M., 2005. Global seismicity of 2002: centroid-moment-tensor solutions for 1034 earthquakes. Physics of the Earth and Planetary Interiors 148, 303–326.

Faccenna, C., Becker, T.W., Lucente, F.P., Jolivet, L., Rossetti, F., 2001. History of subduction and back-arc extension in the central Mediterranean. Geophysical Journal International 145, 809–820. http://dx.doi.org/10.1046/j.0956-540x.2001.01435.x.

Faccenna, C., Piromallo, C., Crespo-Blanc, A., Jolivet, L., 2004. Lateral slab deformation and the origin of the western Mediterranean arcs. Tectonics 23, TC1012. http://dx.doi.org/10.1029/2002TC001488.

Faccenna, C., Civetta, L., D'Antonio, M., Funiciello, F., Margheriti, L., Piromallo, C., 2005. Constraints on mantle circulation around the deforming Calabrian slab. Geophysical Research Letters 32, L06311.

Faccenna, C., Molin, P., Orecchio, B., Olivetti, V., Bellier, O., Funiciello, F., Minelli, L., Piromallo, C., Billi, A., 2011. Topography of the Calabria subduction zone (southern Italy): clues for the origin of Mt Etna. Tectonics 30, TC1003. http://dx.doi.org/10.1029/2010TC002694.

Ferranti, L., Santoro, E., Mazzella, M.E., Monaco, C., Morelli, D., 2009. Active transpression in the Northern Calabria Apennines, Southern Italy. Tectonophysics 476, 226–251.

Finetti, I.R., 2005a. Depth contour map of the moho discontinuity in the central Mediterranean region from new CROP seismic data. In: Finetti, I.R. (Ed.), CROP PROJECT: Deep Seismic Exploration of the Central Mediterranean and Italy. Elsevier, Amsterdam, pp. 597–606.

Finetti, I.R., 2005b. The Calabrian Arc and subducting Ionian slab from the new CROP seismic data. In: Finetti, I.R. (Ed.), CROP PROJECT: Deep Seismic Exploration of the Central Mediterranean and Italy. Elsevier, Amsterdam, pp. 393–412.

Frepoli, A., Amato, A., 2000a. Fault plane solutions of crustal earthquakes in southern Italy (1988–1995) seismotectonic implications. Annali di Geofisica 43, 437–467.

Frepoli, A., Amato, A., 2000b. Spatial variation in stresses in peninsular Italy and Sicily from background seismicity. Tectonophysics 317, 109–124.

Frepoli, A., Cinti, F.R., Amicucci, L., Cimini, G.B., De Gori, P., Pierdominici, S., 2005. Pattern of seismicity in the Lucanian Apennines and foredeep (Southern Italy) from recording by SAPTEX temporary array. Annals of Geophysics 48, 1035–1054.

Frepoli, A., Maggi, C., Cimini, G.B., Marchetti, A., Chiappino, M., 2011. Seismotectonic of Southern Apennines from recent passive seismic experiments. Journal of Geodynamics 51, 110–124.

Galadini, F., Meletti, C., Rebez, A., 2000. (A cura di). Le ricerche del GNDT nel campo della pericolosità sismica (1996–1999). CNR-Gruppo Nazionale per la Difesa dai Terremoti, Roma (397 pp.).

Galli, P., Bosi, V., 2002. Paleoseismology along the Cittanova fault: implications for seismotectonics and earthquake recurrence in Calabria (southern Italy). Journal of Geophysical Research 107, B3. http://dx.doi.org/10.1029/2001JB000234.

Galli, P., Galadini, F., 2003. Disruptive earthquakes revealed by faulted archaeological relics in Samnium (Molise, southern Italy). Geophysical Research Letters 30, 1266. http://dx.doi.org/10.1029/2002GL016456.

Galli, P., Scionti, V., 2006. Two unknown M > 6 historical earthquakes revealed by palaeoseismological and archival researches in eastern Calabria (southern Italy). Seismotectonic implications. Terra Nova 18, 44–49.

Galli, P., Bosi, V., Piscitelli, S., Giocoli, A., Scionti, V., 2006. Late Holocene earthquakes in Southern Apennines: paleoseismology of the Caggiano fault. International Journal of Earth Sciences 95, 855–870.

Galli, P., Galadini, F., Pantosti, D., 2008. Twenty years of paleoseismology in Italy. Earth-Science Reviews 88, 89–117.

Gephart, J.W., 1990. Stress and the direction of slip on fault planes. Tectonics 9, 845–858.

Gephart, J., Forsyth, W., 1984. An improved method for determining the regional stress tensor using earthquake focal mechanism data: application to the San Fernando earthquake sequence. Journal of Geophysical Research 89, 9305–9320.

Giampiccolo, E., Musumeci, C., Falà, F., Gresta, S., 2008. Seismological investigations in the Gioia Tauro Basin (southern Calabria, Italy). Annals of Geophysics 51, 769–799. http://dx.doi.org/10.4401/ag-3018.

Giano, S.I., Maschio, L., Alessio, M., Ferranti, L., Improta, S., Schiattarella, M., 2000. Radiocarbon dating of active faulting in the Agri high valley, southern Italy. Journal of Geodynamics 29, 371–386.

Gillard, D., Wyss, M., Okubo, P., 1996. Type of faulting and orientation of stress and strain as a function of space and time in Kilauea's south flank. Hawaii. Journal of Geophysical Research 101, 16025–16042.

Goes, S., Giardini, D., Jenny, S., Hollenstein, C., Kahle, H.G., Geiger, A., 2004. A recent tectonic reorganization in the south-central Mediterranean. Earth and Planetary Science Letters 226, 335–345.

Govers, R., Wortel, M.J.R., 2005. Lithosphere tearing at STEP faults: response to edges of subduction zones. Earth and Planetary Science Letters 236, 505–523.

Grasso, M., 1993. Pleistocene structures at the Ionian side of the Hyblean Plateau (SE Sicily): implications for the tectonic evolution of the Malta escarpment. In: Max, M.D., Colantoni, P. (Eds.), Geological Development of the Sicilian–Tunisian Platform. Rep. Mar. Sci., 58. UNESCO, Paris, pp. 49–54.

Gresta, S., Patanè, G., 1987. Review of seismological studies at Mount Etna. Pure and Applied Geophysics 125, 951–970. http://dx.doi.org/10.1007/BF00879362.

Gresta, S., Ghisetti, F., Privitera, E., Bonanno, A., 2005. Coupling of eruptions and earthquakes at Mt Etna (Sicily, Italy): a case study from the 1981 and 2001 events. Geophysical Research Letters 32, L05306. http://dx.doi.org/10.1029/2004GL021479.

Grimison, N.L., Chen, W.P., 1986. The Azores-Gibraltar plate boundary —focal mechanisms, depths of earthquakes, and their tectonic implications. Journal of Geophysical Research — Solid Earth and Planets 91 (B2), 2029–2047. http://dx.doi.org/10.1029/JB091iB02p02029.

Gueguen, E., Doglioni, C., Fernandez, M., 1998. On the post-25 Ma geodynamic evolution of the western Mediterranean. Tectonophysics 298, 259–269.

Guidoboni, E., Mariotti, D., Giammarinaro, M.S., Rovelli, A., 2003. Identification of amplified damage zones in Palermo, Sicily (Italy), during the earthquakes of the last three centuries. Bulletin of the Seismological Society of America 93, 1649–1669.

Gutscher, M.A., Roger, J., Baptista, M.A., Miranda, J.M., Tinti, S., 2006. Source of the 1693 Catania earthquake and tsunami (southern Italy): new evidence from tsunami modeling of a locked subduction fault plane. Geophysical Research Letters 33, L08309. http://dx.doi.org/10.1029/2005GL025442.

Gvirtzman, Z., Nur, A., 1999. Plate detachment, asthenosphere upwelling, and topography across subduction zones. Geology 27, 563–566.

Gvirtzman, Z., Nur, A., 2001. Residual topography, lithospheric structure and sunken slabs in the central Mediterranean. Earth and Planetary Science Letters 187, 117–130.

Hollenstein, C.H., Kahle, H.-G., Geiger, A., Jenny, S., Goes, S., Giardini, D., 2003. New GPS constraints on the Africa–Eurasia plate boundary zone in southern Italy. Geophysical Research Letters 30, 1935. http://dx.doi.org/10.1029/2003GL017554.

Improta, L., Ferranti, L., De Martini, P.M., Piscitelli, S., Bruno, P.P., Burrato, P., Civico, R., Giocoli, A., Iorio, M., D'Addezio, G., Maschio, L., 2010. Detecting young, slow-slipping active faults by geologic and multidisciplinary highresolution geophysical investigations: a case study from the Apennine seismic belt, Italy. Journal of Geophysical Research 115, B11307. http://dx.doi.org/10.1029/2010JB000871.

Isacks, B., Molnar, P., 1971. Distribution of stresses in the descending lithosphere from a global survey of focal-mechanism solutions of mantle earthquakes. Reviews of Geophysics and Space Physics 9, 103–174.

Jackson, J., McKenzie, D., 1988. The relationship between plate motions and seismic moment tensors, and the rates of active deformation in the Mediterranean and Middle-East. Geophysical Journal International 93, 45–73.

Jacques, E., Monaco, C., Tapponier, P., Tortorici, L., Winter, T., 2001. Faulting and earthquake triggering during the 1783 Calabria seismic sequence. Geophysical Journal International 147, 499–516.

Kagan, Y.Y., 1991. 3-D rotation of double-couple earthquake sources. Geophysical Journal International 106, 709–716.

Knott, D.S., Turco, E., 1991. Late Cenozoic kinematic of the Calabrian arc, southern Italy. Tectonics 10 (6), 1164–1172.

Lambeck, K., Antonioli, F., Purcell, A., Silenzi, S., 2004. Sea-level change along the Italian coast for the past 10,000 yr. Quaternary Science Reviews 23 (14–15), 1567–1598. http://dx.doi.org/10.1016/j.quascirev.2004.02.009.

Lavecchia, G., Ferrarini, F., de Nardis, R., Visini, F., Barbano, M.S., 2007a. Active thrusting as a possible seismogenic source in Sicily (southern Italy): some insights from integrated structural-kinematic and seismological data. Tectonophysics 445, 145–167. http://dx.doi.org/10.1016/j.tecto.2007.07.007.

Lavecchia, G., de Nardis, R., Visini, F., Ferrarini, F., Barbano, M.S., 2007b. Seismogenic evidence of ongoing compression in eastern-central Italy and mainland Sicily: a comparison. Italian Journal of Geosciences 126, 209–222.

Lay, T., Wallace, T.C., 1995. Modern Global Seismology. Academic Press, San Diego.

Li, H., Michelini, A., Zhu, L., Bernardi, F., Spada, M., 2007. Crustal velocity structure in Italy from analysis of regional seismic waveforms. Bulletin of the Seismological Society of America 97, 2024–2039. http://dx.doi.org/10.1785/0120070071.

Lindholm, C.D., Bungum, H., Bratli, R.K., Aadnøy, B.S., Dahl, N., Tørudbakken, B., Atakan, K., 1995. Crustal stress in the northern North Sea as inferred from borehole breakouts and earthquake focal mechanisms. Terra Nova 7, 51–59.

Lucente, F.P., Margheriti, L., Piromallo, C., Barruol, G., 2006. Seismic anisotropy reveals the long route of the slab through the western central Mediterranean mantle. Earth and Planetary Science Letters 241, 517–529.

Lustrino, M., Duggen, S., Rosenberg, C.L., 2011. The Central-Western Mediterranean: anomalous igneous activity in an anomalous collisional tectonic setting. Earth-Science Reviews 104 (1–3), 1–40. http://dx.doi.org/10.1016/j.earscirev.2010.08.002.

Maggi, C., Frepoli, A., Cimini, G.B., Console, R., Chiappini, M., 2009. Recent seismicity and crustal stress field in the Lucanian Apennines and surrounding areas (Southern Italy): seismotectonic implications. Tectonophysics 463, 130–144.

Malinverno, A., Ryan, W., 1986. Extension in the Tyrrhenian Sea and shortening in the Apennines as result of arc migration driven by sinking of the lithosphere. Tectonics 5, 227–245.

Mandle, G., 1988. Mechanics of tectonic faulting: models and basic concepts. In: Zwart, H.J. (Ed.), Developments in Structural Geology. Elsevier, Amsterdam, p. 407.

Mariotti, G., Doglioni, C., 2000. The dip of the foreland monocline in the Alps and Apennines. Earth and Planetary Science Letters 181, 191–202.

Maschio, L., Ferranti, L., Burrato, P., 2005. Active extension in Val d'Agri area, Southern Apennines, Italy: implications for the geometry of the seismogenic belt. Geophysical Journal International 162, 591–609.

Mattei, M., Petrocelli, V., Lacava, D., Schiattarella, M., 2004. Geodynamic implications of Pleistocene ultrarapid vertical-axis rotations in the Southern Apennines, Italy. Geology 32, 789–792.

Mattei, M., Cifelli, F., D'Agostino, N., 2007. The evolution of the Calabrian Arc: evidence from paleomagnetic and GPS observations. Earth and Planetary Science Letters 263, 259–274.

McCaffrey, R., Molnar, P., Roecker, S., Joyodiwiryo, Y., 1985. Microearthquake seismicity and fault plane solutions related to arc-continent collision in the Eastern Sunda Arc, Indonesia. Journal of Geophysical Research 90, 4511–4528.

McKenzie, D., 1969. The relationship between fault plane solutions for earthquakes and the directions of the principal stresses. Bulletin of the Seismological Society of America 59, 591–601.

Miller, M.S., Piana Agostinetti, N., 2011. Erosion of the continental lithosphere at the cusps of the Calabrian arc: evidence from S receiver functions analysis. Geophysical Research Letters 38. http://dx.doi.org/10.1029/2011GL049455.

Minelli, L., Faccenna, C., 2010. Evolution of the Calabrian accretionary wedge (central Mediterranean). Tectonics 29, TC4004. http://dx.doi.org/10.1029/2009TC002562.

Molin, P., Pazzaglia, F.J., Dramis, F., 2004. Geomorphic expression of active tectonics in a rapidly-deforming forearc, Silamassif, Calabria, southern Italy. American Journal of Science 304, 559–589.

Monaco, C., Tortorici, L., 2000. Active faulting in the Calabrian arc and eastern Sicily. Journal of Geodynamics 29, 407–424.

Monaco, C., Mazzoli, S., Tortorici, L., 1996. Active thrust tectonics in western Sicily (southern Italy): the 1968 Belice earthquake sequence. Terra Nova 8, 372–381.

Montone, P., Mariucci, M.T., Pondrelli, S., Amato, A., 2004. An improved stress map for Italy and surrounding regions (central Mediterranean). Journal of Geophysical Research 109, B10410. http://dx.doi.org/10.1029/2003JB002703.

Montuori, C., Cimini, G.B., Favali, P., 2007. Teleseismic tomography of the southern Tyrrhenian subduction zone: new results from seafloor and land recordings. Journal of Geophysical Research 112, B03311.

Moro, M., Amicucci, L., Cinti, F.R., Doumaz, F., Montone, P., Pierdominici, S., Saroli, M., Stramondo, S., Di Fiore, B., 2007. Surface evidence of active tectonics along the Pergola-Melandro fault: a critical issue for the seismogenic potential of the southern Apennines, Italy. Journal of Geodynamics 44, 19–32.

Musumeci, C., Patane, D., Scarfì, L., Gresta, S., 2005. Stress directions and shear-wave anisotropy: observations from local earthquakes in southeastern Sicily, Italy. Bulletin of the Seismological Society of America 95 (4), 1359–1374. http://dx.doi.org/10.1785/0120040108.

Negredo, A.M., Sabadini, R., Bianco, G., Fernandez, M., 1999. Three-dimensional modelling of crustal motions caused by subduction and continental convergence in the central Mediterranean. Geophysical Journal International 136, 261–274.

Neri, G., Barberi, G., Orecchio, B., Aloisi, M., 2002. Seismotomography of the crust in the transition zone between the southern Tyrrhenian and Sicilian tectonic domains. Geophysical Research Letters 29, 23. http://dx.doi.org/10.1029/2002GL015562, 2002.

Neri, G., Barberi, G., Orecchio, B., Mostaccio, A., 2003. Seismic strain and seismogenic stress regimes in the crust of the southern Tyrrhenian region. Earth and Planetary Science Letters 213, 97–112.

Neri, G., Barberi, G., Oliva, G., Orecchio, B., 2004. Tectonic stress and seismogenic faulting in the area of the 1908 Messina earthquake, south Italy. Geophysical Research Letters 31, 10. http://dx.doi.org/10.1029/2004GL019742.

Neri, G., Barberi, G., Oliva, G., Orecchio, B., 2005. Spatial variations of seismogenic stress orientations in Sicily, south Italy. Physics of the Earth and Planetary Interiors 148, 175–191.

Neri, G., Oliva, B., Orecchio, B., Presti, D., 2006. A possible seismic gap within a highly seismogenic belt crossing Calabria and eastern Sicily, Italy. Bulletin of the Seismological Society of America 96, 321–331.

Neri, G., Orecchio, B., Presti, D., 2008. Sismicità attuale, campo di sforzo e dinamiche litosferiche nell'area dello Stretto di Messina. In: Bertolaso, G., Boschi, E., Guidoboni, E., Valensise, G. (Eds.), Il terremoto e il maremoto del 28 dicembre 1908: INGV-SGA, pp. 461–474.

Neri, G., Orecchio, B., Totaro, C., Falcone, G., Presti, D., 2009. Seismic tomography says that lithospheric subduction beneath south Italy is close to die. Seismological Research Letters 80, 63–70. http://dx.doi.org/10.1785/gssrl.80.1.63.

Nocquet, J.-M., Calais, E., 2004. Geodetic measurements of crustal deformation in the Western Mediterranean and Europe. Pure and Applied Geophysics 161, 661–681. http://dx.doi.org/10.1007/s00024-003-2468-z.

Olivetti, V., Balestrieri, M.L., Faccenna, C., Stuart, F.M., Vignaroli, G., 2010. Middle Miocene out-of-sequence thrusting and successive exhumation in the Peloritani Mountains, Sicily: late stage evolution of an orogen unraveled by apatite fission track and (U-Th)/He thermochronometry. Tectonics 29, TC5005. http://dx.doi.org/10.1029/2009TC002659.

Olivetti, V., Cyr, A.J., Molin, P., Faccenna, C., Granger, D.E., 2012. Uplift history of the Sila Massif, southern Italy, deciphered from cosmogenic ^{10}Be erosion rates and river longitudinal profile analysis. Tectonics 31, TC3007. http://dx.doi.org/10.1029/2011TC003037.

Orecchio, B., Presti, D., Totaro, C., Guerra, I., Neri, G., 2011. Imaging the velocity structure of the Calabrian Arc region (South Italy) through the integration of different seismological data. Bollettino di Geofisica Teorica ed Applicata 52, 625–638.

Palano, M., Cannavò, F., Ferranti, L., Mattia, M., Gazzella, M.E., 2011. Strain and stress fields in the Southern Apennines (Italy) constrained by geodetic, seismological and borehole data. Geophysical Journal International. http://dx.doi.org/10.1111/j.1365-246X.2011.05234.x.

Palano, M., Ferranti, L., Monaco, C., Mattia, M., Aloisi, M., Bruno, V., Cannavò, F., Siligato, G., 2012. GPS velocity and strain fields in Sicily and southern Calabria, Italy: updated geodetic constraints on tectonic block interaction in the central Mediterranean. Journal of Geophysical Research 117, B07401. http://dx.doi.org/10.1029/2012JB009254.

Pantosti, D., Valensise, G., 1990. Faulting mechanism and complexity of the Novembre 23, 1980, Campania–Lucania Earthquake, inferred from surface observation. Journal of Geophysical Research 95 (B10), 15319–15341.

Pantosti, D., Schwartz, D., Valensise, G., 1993. Paleoseismology along the 1980 surface rupture in Irpinia Fault: implications for earthquake recurrence in the Southern Apennines, Italy. Journal of Geophysical Research 98 (4), 6561–6577.

Papanikolaou, I.D., Roberts, G.P., 2007. Geometry, kinematics and deformation rates along the active normal fault system in the southern Apennines: implication for fault growth. Journal of Structural Geology 29, 166–188.

Parker, R.L., McNutt, M.K., 1980. Statistics for the one-norm misfit measure. Journal of Geophysical Research 85, 4429–4430.

Pasquale, G., De Matteis, R., Romeo, A., Maresca, R., 2009. Earthquake focal mechanisms and stress inversion in the Irpinia Region (Southern Italy). Journal of Seismology 13, 107–124. http://dx.doi.org/10.1007/s10950-008-9119-x.

Patacca, E., Scandone, P., 2007. Geological interpretation of the CROP-04 seismic line (southern Apennines, Italy). Boll. Soc. Geol. It. (Ital. J. Geosci.), special issue n°7, pp. 297–315.

Patanè, D., De Gori, P., Chiarabba, C., Bonaccorso, A., 2003. Magma ascent and the pressurization of Mount Etna's volcanic system. Science 299, 2061–2063. http://dx.doi.org/10.1126/science.1080653.

Peccerillo, A., 2003. Plio-Quaternary magmatism in Italy. Episodes 26, 222–226.

Pepe, F., Bertotti, G., Cella, F., Marsella, E., 2000. Rifted margin formation in the south Tyrrhenian Sea: a high-resolution seismic profile across the north Sicily passive continental margin. Tectonics 19, 241–257.

Pepe, F., Sulli, A., Bertotti, G., Catalano, R., 2005. Structural highs formation and their relationship to sedimentary basins in the north Sicily continental margin (southern Tyrrhenian Sea): implication for the Drepano Thrust Front. Tectonophysics 409, 1–18. http://dx.doi.org/10.1016/j.tecto.2005.05.009.

Pepe, F., Sulli, A., Bertotti, G., Cella, F., 2010. Architecture and Neogene to Recent evolution of the western Calabrian continental margin: An upper plate perspective to the Ionian subduction system, central Mediterranean. Tectonics 29, TC3007. http://dx.doi.org/10.1029/2009TC002599.

Piana Agostinetti, N., Amato, A., 2009. Moho depth and Vp/Vs ratio in peninsular Italy from teleseismic receiver functions. Journal of Geophysical Research 114, B06303. http://dx.doi.org/10.1029/2008JB005899.

Pierdominici, S., Heidbach, O., 2012. Stress field of Italy — mean stress orientation at different depths and wave-length of the stress pattern. Tectonophysics 532, 301–311. http://dx.doi.org/10.1016/j.tecto.2012.02.018.

Pino, N., Piatanesi, A., Valensise, G., Boschi, E., 2009. The 28 December 1908 Messina Straits earthquake (Mw 7.1): a great earthquake throughout a century of seismology. Seismological Research Letters 80, 243–259.

Piromallo, C., Becker, T.W., Funiciello, F., Faccenna, C., 2006. Three-dimensional instantaneous mantle flow induced by subduction. Geophysical Research Letters 33, L08304. http://dx.doi.org/10.1029/2005GL025390.

Polonia, A., Torelli, L., Mussoni, P., Gasperini, L., Artoni, A., Klaeschen, D., 2011. The Calabrian Arc subduction complex I the Ionian Sea: regional architecture, active deformation, and seismic hazard. Tectonics 30, TC5018. http://dx.doi.org/10.1029/2010TC002821.

Polonia, A., Torelli, L., Gasperini, L., Mussoni, P., 2012. Active faults and historical earthquakes in the Messina Straits area (Ionian Sea). Natural Hazards and Earth System Sciences 12. http://dx.doi.org/10.5194/nhess-12-1-2012.

Pondrelli, S., Morelli, A., Ekstrom, G., Mazza, S., Boschi, E., Dziewonski, A.M., 2002. European–Mediterranean regional centroid-moment tensors: 1997–2000. Physics of the Earth and Planetary Interiors 130 (1–2), 71–101.

Pondrelli, S., Morelli, A., Ekstrom, G., 2004a. European–Mediterranean regional centroid-moment tensor catalog: solutions for years 2001 and 2002. Physics of the Earth and Planetary Interiors 145 (1–4), 127–147.

Pondrelli, S., Piromallo, C., Serpelloni, E., 2004b. Convergence vs. retreat in Southern Tyrrhenian Sea: insights from kinematics. Geophysical Research Letters 31 (6), L06611.

Pondrelli, S., Salimbeni, S., Ekstrom, G., Morelli, A., Gasperini, P., Vannucci, G., 2006. The Italian CMT dataset from 1977 to the present. Physics of the Earth and Planetary Interiors 159 (3–4), 286–303.

Pondrelli, S., Salimbeni, S., Morelli, A., Ekström, G., Boschi, E., 2007. European–mediterranean regional centroid moment tensor catalog: solutions for years 2003 and 2004. Physics of the Earth and Planetary Interiors 164 (1–2), 90–112.

Pondrelli, S., Salimbeni, S., Morelli, A., Ekström, G., Postpischl, L., Vannucci, G., Boschi, E., 2011. European–Mediterranean Regional Centroid Moment Tensor catalog: solutions for 2005–2008. Physics of the Earth and Planetary Interiors 185 (3–4), 74–81.

Presti, D., Orecchio, B., Falcone, G., Neri, G., 2008. Linear versus non-linear earthquake location and seismogenic fault detection in the southern Tyrrhenian Sea, Italy. Geophysical Journal International 172, 607–618.

Reitz, M.A., Seeber, L., 2012. Arc-parallel strain in a short rollback-subduction system: the structural evolution of the Crotone basin (northeastern Calabria, Southern Italy). Tectonics 31 (23), TC4017. http://dx.doi.org/10.1029/2011TC003031.

Rosenbaum, G., Lister, G.S., 2004. Neogene and Quaternary rollback evolution of the Tyrrhenian sea, the Apennines, and the Sicilian Maghrebides. Tectonics 23, TC1013. http://dx.doi.org/10.1029/2003TC001518.

Rosenbaum, G., Gasparon, M., Lucente, F.P., Peccerillo, A., Miller, M.S., 2008. Kinematics of slab tear faults during subduction segmentation and implications for Italian magmatism. Tectonics 27, TC2008. http://dx.doi.org/10.1029/2007TC002143.

Ryan, W.B.F., Heezen, B.C., 1965. Ionian Sea submarine canyons and the 1908 Messina turbidity current. Geological Society of America Bulletin 76, 915–932.

Scognamiglio, L., Tinti, E., Michelini, A., 2009. Real-time determination of seismic moment tensor for the Italian Region. Bulletin of the Seismological Society of America 99 (4), 2223–2242. http://dx.doi.org/10.1785/0120080104.

Scognamiglio, L., Tinti, E., Michelini, A., 2010. Fast determination of moment tensors and rupture history: what has been learned from the 6 April 2009 L'Aquila Earthquake sequence. Seismological Research Letters 81 (6), 892–906. http://dx.doi.org/10.1785/gssrl.81.6.892.

Scrocca, D., Carminati, E., Doglioni, C., 2005. Deep structure of the southern Apennines, Italy: thin-skinned or thick-skinned? Tectonics 24, TC3005. http://dx.doi.org/10.1029/2004TC001634.

Scrocca, D., Sciamanna, S., Di Luzio, E., Tozzi, M., Nicolai, C., Gambini, R., 2007. Structural setting along the CROP-04 deep seismic profile (Southern Apennines — Italy). Boll.Soc.Geol.It. (Ital.J.Geosci.), Spec. Issue No. 7, pp. 283–296.

Seeber, L., Reitz, M., Nagel, T., Steckler, M., 2008. Collision versus separation in rollback: the Calabria Arc through the Apulia-Africa narrow. EOS. Transactions of the American Geophysical Union 89 (53) (Fall Meet. Suppl., Abstract T53B-1934).

Sella, G.F., Dixon, T.H., Mao, A., 2002. REVEL: a model for recent plate velocities from space geodesy. Journal of Geophysical Research 107. http://dx.doi.org/10.1029/2000JB000033.

Selvaggi, G., Chiarabba, C., 1995. Seismicity and P wave velocity image of the southern Tyrrhenian subduction zone. Geophysical Journal International 121, 818–826. http://dx.doi.org/10.1111/j.1365-246X.1995.tb06441.x.

Serpelloni, E., Vannucci, G., Pondrelli, S., Argnani, A., Casula, G., Anzidei, M., Baldi, P., Gasperini, P., 2007. Kinematics of the western Africa–Eurasia plate boundary from local machanisms and GPS data. Geophysical Journal International 169, 1180–1200.

Serpelloni, E., Bürgmann, R., Anzidei, M., Baldi, P., Mastrolembo Ventura, B., Boschi, E., 2010. Strain accumulation across the Messina Straits and kinematics of Sicily and Calabria from GPS data and dislocation modeling. Earth and Planetary Science Letters 298, 1–14.

Sgroi, T., de Nardis, R., Lavecchia, G., 2012. Crustal structure and seismotectonics of central Sicily (southern Italy): new constraints from instrumental seismicity. Geophysical Journal International 189 (3), 1237–1252. http://dx.doi.org/10.1111/j.1365-246X.2012.05392.x.

Sirovich, L., Pettenati, F., 2001. Test of source-parameter of the intensities of a 54,000-death shock of the seventeenth century in southeast Sicily. Bulletin of the Seismological Society of America 91, 792–811.

Spakman, W., Wortel, R., 2004. A tomographic view on western Mediterranean geodynamics. In: Cavazza, W. (Ed.), The Transmed Atlas: The Mediterranean Region from Crust to Mantle. Springer, New York, pp. 31–52.

Speranza, F., Maniscalco, R., Mattei, M., Di Stefano, A., Butler, R.W.H., Funiciello, R., 1999. Timing and magnitude of rotations in the frontal thrust systems of southwestern Sicily. Tectonics 18, 1178–1197.

Speranza, F., Macrì, P., Rio, D., Fornaciari, E., Consolaro, C., 2011. Paleomagnetic evidence for a post-1.2 Ma disruption of the Calabria terrane: consequences of slab breakoff on orogenic wedge tectonics. Geological Society of America Bulletin 123, 925–933.

Spina, V., Tondi, E., Galli, P., Mazzoli, S., Cello, G., 2008. Quaternary fault segmentation and interaction in the epicentral area of the 1561 earthquake (Mw = 6.4), Vallo di Diano, southern Apennines, Italy. Tectonophysics 453, 233–245.

Spina, V., Tondi, E., Galli, P., Mazzoli, S., 2009. Fault propagation in a seismic gap area (northern Calabria, Italy): implications for seismic hazard. Tectonophysics 476, 357–369.

Spina, V., Tondi, E., Mazzoli, S., 2011. Complex basin development in a wrench-dominated back-arc area: tectonic evolution of the Crati basin, Calabria, Italy. Journal of Geodynamics 51, 90–109.

Steckler, M.S., Piana Agostinetti, N., Wilson, C.K., Roselli, P., Seeber, L., Amato, A., Lerner-Lam, A., 2008. Crustal structure in the Southern Apennines from teleseismic receiver functions. Geology 36, 155–158.

Sykes, L.R., 1967. Mechanism of earthquakes and nature of faulting on the mid-oceanic ridges. Journal of Geophysical Research 72, 5–27.

Tan, Y., Zhu, L., Helmberger, D., Saikia, C., 2006. Locating and modeling regional earthquakes with two stations. Journal of Geophysical Research 111, B01306.

Tansi, C., Muto, F., Critelli, S., Iovine, G., 2007. Neogene–Quaternary strike-slip tectonics in the central Calabrian Arc (southern Italy). Journal of Geodynamics 43, 393–414.

Tortorici, L., Monaco, C., Tansi, C., Cocina, O., 1995a. Recent and active tectonics in the Calabrian Arc (southern Italy). Tectonophysics 243, 7–55.

Tortorici, L., Ventura, G., Mazzuoli, R., Monaco, C., 1995b. Strutture del settore orientale dell'Arcipelago Eoliano: interpretazione tettonica e modellizzazione numerica. Studi Geologici Camerti 1995 (2), 455–466.

Townend, J., Zoback, M.D., 2006. Stress, strain, and mountain building in central Japan. Journal of Geophysical Research 111, B03411. http://dx.doi.org/10.1029/2005JB003759.

Valensise, L., Pantosti, D., 1992. A 125 kyr-long geological record of seismic source repeatability: the Messina Straits (southern Italy) and the 1908 earthquake (Ms = 71/2). Terra Nova 4, 472–483.

Valoroso, L., Improta, L., Chiaraluce, L., Di Stefano, R., Ferranti, L., Govoni, A., Chiarabba, C., 2009. Active faults and induced seismicity in the Val d'Agri area (Southern Apennines, Italy). Geophysical Journal International 178, 488–502.

Valoroso, L., Improta, L., De Gori, P., Chiarabba, C., 2011. Upper crustal structure, seismicity and pore pressure variations in an extensional seismic belt through 3-D and 4-D V_P and V_P/V_S models: the example of the Val d'Agri area (southern Italy). Journal of Geophysical Research 116, B07303. http://dx.doi.org/10.1029/2010JB007661.

Van Dijk, J.P., 1994. Late Neogene kinematics of intra-arc oblique shear zones: the Petilia–Rizzuto Fault Zone (Calabrian Arc, central Mediterranean). Tectonics 13, 1201–1230.

Vannucci, G., Gasperini, P., 2004. The new release of the database of Earthquake Mechanisms of the Mediterranean Area (EMMA Version 2). Annals of Geophysics 47 (1), 307–334.

Vignaroli, G., Rossetti, F., Theye, T., Faccenna, C., 2008. Styles and regimes of orogenic thickening in the Peloritani Mountains (Sicily, Italy): new constraints on the tectono-metamorphic evolution of the Apennine belt. Geological Magazine 145, 552–569.

Villani, F., Pierdominici, S., 2010. Late Quaternary tectonics of the Vallo di Diano basin (southern Apennines, Italy). Quaternary Science Reviews 1–17. http://dx.doi.org/10.1016/j.quascirev.2010.07.003.

Visini, F., De Nardis, R., Barbano, M.S., Lavecchia, G., 2009. Testing the seismogenic sources of the January 11th 1693 Sicilian earthquake (I0 X/XI): insights from macroseismic field simulations. Italian Journal of Geosciences 128, 147–156.

Visini, F., de Nardis, R., Lavecchia, G., 2010. Rates of active compressional deformation in central Italy and Sicily: evaluation of the seismic budget. International Journal of Earth Sciences 99, S243–S264. http://dx.doi.org/10.1007/s00531-009-0473-x.

Westaway, R., Jackson, J., 1984. Surface faulting in the Southern Italian Campania–Basilicata earthquake of 23 November 1980. Nature 312, 436–438.

Wilson, J.T., 1965. A new class of faults and their bearing on continental drift. Nature 207, 343–347.

Wortel, M.J.R., Spakman, W., 2000. Subduction and slab detachment in the Mediterranean–Carpathian region. Science 290, 1910–1917.

Wyss, M., Liang, B., Tanigawa, W.R., Xiaoping, W., 1992. Comparison of orientations of stress and strain tensor based on fault plane solutions in Kaoiki, Hawaii. Journal of Geophysical Research 97, 4769–4790.

Zhao, L.S., Helmberger, D., 1994. Source estimation from broad-band regional seismograms. Bulletin of the Seismological Society of America 85, 590–605.

Zhu, L., Helmberger, D., 1996. Advancement in source estimation technique using broadband regional seismograms. Bulletin of the Seismological Society of America 86, 1634–1641.

Zhu, L., Akyol, N., Mitchell, B., Sozbiliz, H., 2006. Seismotectonics of western Turkey from high resolution and moment tensor determinations. Geophysical Research Letters 33, L07316. http://dx.doi.org/10.1029/2006GL025842.

Zoback, M.D., 1983. State of stress in the lithosphere. Reviews of Geophysics 21, 1503–1511.

Zoback, M.L., 1992. First- and second-order patterns of stress in the lithosphere: the World Stress Map project. Journal of Geophysical Research 97 (11), 703–711 (728).

Zoback, M., Zoback, M., 1980. State of stress in the conterminous United States. Journal of Geophysical Research 85, 6113–6156.